AGU PUBLICATIONS

Water Resources Research

RESEARCH ARTICLE
10.1002/2015WR017485

Dynamic, structured heterogeneity of water isotopes inside hillslopes

Jasper Oshun[1], William E. Dietrich[2], Todd E. Dawson[3], and Inez Fung[2]

[1]Department of Geology, Humboldt State University, Arcata, California, USA, [2]Department of Earth and Planetary Science, University of California, Berkeley, Berkeley, California, USA, [3]Department of Integrative Biology, University of California, Berkeley, Berkeley, California, USA

Key Points:
- Material properties in the subsurface impart an isotopic "fingerprint" on their waters
- A structured heterogeneity of water isotopes persists in the subsurface of the critical zone
- We sample deeply and frequently to characterize water isotopes for ecohydrologic tracers

Supporting Information:
- Supporting Information S1
- Data Set S1

Correspondence to:
J. Oshun,
oshun@humboldt.edu

Citation:
Oshun, J., W. E. Dietrich, T. E. Dawson, and I. Fung (2015), Dynamic, structured heterogeneity of water isotopes inside hillslopes, *Water Resour. Res.*, *51*, doi:10.1002/2015WR017485.

Received 29 MAY 2015
Accepted 2 DEC 2015
Accepted article online 9 DEC 2015

Abstract Use of the stable isotopes of water (δD, δ^{18}O) to determine vegetative water sources, runoff paths, and residence times generally assumes that, other than shallow evaporative enrichment, the isotopic composition of precipitation is conserved as it travels through the subsurface to the stream channel. Here we follow rainfall through a thick (up to 25m) vadose zone of soil, saprolite, and weathered bedrock mostly composed of argillite, and underlying a steep (32°) forested hillslope. We discover a persistent structured heterogeneity of water isotopes inside the hillslope. Summer dry season causes evaporative enrichment of the soil, but not in the saprolite and weathered bedrock. In winter, the mobile water, generated by successive rainstorms with widely varying isotopic composition, mixes in the vadose zone, elevating soil and rock moisture content, and eventually recharging the groundwater with isotopically invariant water similar to the seasonally averaged rainfall. Yet throughout the winter the less mobile winter soil and rock moisture remains relatively light, and water extracted from the interior of argillite lies well to the left of the local meteoric water line. This persistently light composition of soil and rock moisture and the deviation from average meteoric values suggest that subsurface fractionation, or the inheritance of paleo-meteoric rock moisture associated with rock uplift may lead to large enduring isotopic differences between high and low mobility water. These differences suggest that the use of water isotopes as tracers must consider the possibility of subsurface isotopic evolution and the influence of exchange with more tightly held water.

1. Introduction

Hillslope hydrology studies that employ stable isotope analyses have commonly divided the major water reservoirs into precipitation, soil water, groundwater, stream flow, and if it is a focus of research, vegetation. A central assumption in the use of stable isotopes in hydrological investigations is that, apart from near-surface evaporative effects, the stable isotopes D and ^{18}O act as conservative tracers. This means that by tracking the incoming signal from precipitation, the outflow signal in rivers, and the concentration in various flow components in the soil and in the groundwater, the path, flux rates and residence times of water through the hillslope can be diagnosed [e.g., *Klaus and McDonnell*, 2013; *Kendall et al.*, 2014]. Publications abound, including examples of particular relevance to this study, on the isotopic techniques to define deep and shallow sources contributing to stream flow [e.g., *Anderson et al.*, 1997; *Darling et al.*, 2003; *Banks et al.*, 2009; *Bestland et al.*, 2009; *Gabrielli*, 2011] and the identification of the relative contribution of "old" and "new" water in runoff [e.g., *Sklash and Farvolden*, 1979, *McCaig*, 1983, *Pearce et al.*, 1986; *Sklash et al.*, 1986; *McDonnell*, 1990; *Buttle*, 1994; *Ichiyanagi et al.*, 1994; *Buttle*, 1998; *Zhao et al.*, 2013; *Klaus and McDonnell*, 2013]. An analysis of the stable isotope composition of plant water has been widely used to identify their water source (i.e., which water reservoir is being tapped) [e.g., *Dawson et al.*, 2002; *Evaristo et al.*, 2015].

Two linked elements are missing in many of these studies which we address in the study presented here: (i) the importance on many hillslopes underlain by bedrock of a deep vadose zone extending well below the soil, and (ii) the possibility that in such environments stable isotopes may not act as conservative tracers, i.e., there may be exchange processes between water of variable mobility and the soil and bedrock materials. Many recent studies now show that newly arriving storm water may pass through a relatively thick (~2–20 m) unsaturated weathered bedrock zone (not just the soil) before recharging a perched groundwater aquifer through which runoff is conveyed to channels [e.g., *Wilson and Dietrich*, 1987; *Montgomery et al.*, 1997; *Onda et al.*, 2001; *Tromp-van Meerveld et al.*, 2007; *Kosugi et al.*, 2008; *Katsuyama et al.*, 2010; *Salve*

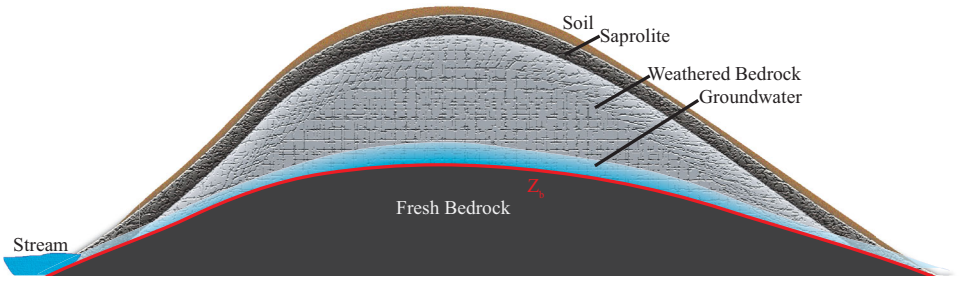

Figure 1. A generalized cross section through a hillslope underlain by bedrock, showing soil, saprolite (soil-like material with a relict rock structure), weathered bedrock and fresh bedrock, and the perching of groundwater on the boundary with fresh bedrock, Zb. The thickness of the mobile upper layer of soil is exaggerated for clarity. Seasonal drainage of the water table to Z_b allows for oxygenation and chemical weathering. Below the minimum water table is fresh bedrock.

et al., 2012]. Although studies have measured the isotopic composition of outflow to infer residence times and pathways of water movement through a hillslope [e.g., *Maloszewski et al*., 1983, 1992; *DeWalle et al*., 1988; *Vitvar and Balderer*, 1997; *Soulsby et al*., 2000; *Asano et al*., 2002; *McGuire et al*., 2002; *Katsuyama et al*., 2010], little is known regarding the isotopic evolution of water as it passes through thick weathering zones of different materials. The tortuous pathways water travels through the hillslope will lead to ample opportunities for exchange between various subsurface reservoirs, which in turn have the potential to alter the isotopic composition of original precipitation inputs before this water becomes runoff in streams. A difference in the isotopic composition of pore waters across glacial tills of different lithologies [*Hiscock et al*., 2011], for example, suggests that material properties may alter the isotopic composition of meteoric waters. Despite the fact that there is support for this notion we found few, if any, studies either acknowledging, or better quantifying the magnitude of such subsurface isotope effects.

The aforementioned studies suggest that we should be looking deeper into hillslopes, and more carefully at reservoirs beyond the soil mantle (which may only be centimeters thick, while the entire "critical zone" [e.g., *Anderson et al*., 2007; *Brantley et al*., 2007; *Jin et al*., 2011; *Rempe and Dietrich*, 2014] may be tens of meters thick) to understand water isotopic evolution. Landscapes are commonly composed of hillslopes bordered by a network of channels. A slice across a hillslope from channel to channel would reveal a layered system: soil, saprolite, weathered bedrock, and fresh bedrock. Under any specific hillslope the presence and thickness of these layers will vary. A generic hillslope is shown in Figure 1. The soil is the skin of the hillslope, a dilationally disturbed mobile upper layer that is composed of organic and mineral material. Below the soil is the immobile saprolite, a soil-like material that retains a relict rock structure despite extensive weathering (sometimes defined by the relatively low abundance of corestones) [e.g., *Green et al*., 2006; *Dixon et al*., 2009]. Weathered bedrock is typically mechanically harder than saprolite, shows signs of mechanical and chemical alteration, and still contains opened interconnected fractures that provide pathways for runoff generation. Typically fracture density decreases with depth [e.g., *Bornyasz et al*., 2005; *Montgomery et al*., 1997; *Salve et al*., 2012]. The elevation at the transition to fresh bedrock (Z_b) [*Rempe and Dietrich*, 2014] may record a significant decrease in hydraulic conductivity such that vertically penetrating storm precipitation will perch and flow laterally to the channel as groundwater flow [e.g., *Salve et al*., 2012], (Figure 1). Dynamic groundwater may also develop in the fresh bedrock. Extending from the soil to this groundwater will be a seasonally dynamic, spatially varying and relatively thick vadose zone.

What lies inside an individual hillslope varies. Hillslopes may lack a soil or saprolite and have only a thin weathered bedrock surface, or, at the other extreme have a saprolite layer that extends the full relief of the hillslope. We suggest that this conceptual structure of what lies inside a hillslope can be used to guide sampling and analysis of water isotopes and mapping across different materials.

Within these four material layers, water can be relatively "mobile" or to varying degrees be tightly held. The concept of mobile and immobile waters in the vadose zone has been extensively explored since initial observations were made by *Biggar and Nielsen* [1962], and *Van Genuchten and Wierenga* [1976] introduced their mobile-immobile conceptual model (MIM) [e.g., *Russo et al*., 1989; *Mayer et al*., 2008]. In essence these studies have shown that water in the vadose zone can be conceived of as stagnant regions of relatively immobile water bounded by pores (or fractures) through which water flow can be rapid. Importantly, these

studies show that solute exchange between the mobile and stagnant water takes place. The proportion of immobile water increases with decreasing water content. The MIM model has been applied extensively to granular soils, and may have application in the more structured materials of saprolite and weathered bedrock [*Šimunek et al*., 2003; *Chen et al*., 2009; *Wang et al*., 2015]. Fracture flow theory, which likely predominates in saprolite and weathered bedrock in many cases, has also conceived of a less mobile water that is held near the boundary and can exchange with more rapidly flowing flow [e.g., *Tokunaga and Wan*, 1997; *Nimmo*, 2010; *Bodin* 2003*; Rosenbom*, 2005; *Neretnieks et al*., 2006].

In our study of hillslope water reservoirs we will make the distinction by apparent mobility. Vadose zone water that transits fairly quickly even as unsaturated flow can be considered mobile and can be operationally defined as water readily extracted by lysimeters under modest tension. These waters move through macropores and fractures and generate runoff. The groundwater would also constitute mobile water. Water obtained by extraction from bulk samples may include everything from highly mobile to tightly held waters, but in drier periods should represent only the more tightly held water associated with the lower soil, saprolite, and weathered bedrock matrix potentials and lower moisture contents. Generally we can refer to these bulk sampled waters as "soil moisture" and "rock moisture" (for bulk samples taken of the saprolite and weathered bedrock and fresh bedrock [*sensu Salve et al*., 2012]). These bulk samples will contain water that ranges from easily displaced to tightly held within micropores. Hence the extraction procedure for sampling will define which waters are included in isotopic analyses [e.g., *Walker et al*., 1994].

Our study is directed at exploring what controls the subsurface isotopic evolution of mobile water and the residual (more tightly held) water in distinct material reservoirs in the subsurface. We hypothesized that the different components of the "subsurface critical zone" (soil, saprolite, weathered bedrock, and mobile water) might have water of different isotopic compositions. Our methods were designed to monitor the isotopic composition of the waters found in each of these reservoirs as well as the mobile waters moving through the hillslope. We describe, for the first time, a persistent structured heterogeneity in the H and O isotope composition of water inside a hillslope and across the entire subsurface critical zone of an actively uplifting and eroding hillslope within the northern California Coast Range. We directly measure water derived from the following mobile reservoirs: precipitation, lysimeter extracted soil and saprolite water, groundwater, and stream water, as well as bulk water within the following subsurface materials: soil, saprolite, weathered bedrock, and fresh bedrock. Our observations reveal that bulk moisture in the soil, saprolite, weathered bedrock, and even the chronically saturated fresh bedrock, is isotopically more negative relative to the mobile water that transits through the hillslope. The persistence of this isotopic offset between bulk and mobile moisture demands a consideration of potential isotope effects that alter the isotopic composition of meteoric water transiting through and recharging the unsaturated and saturated zones inside a hillslope. This has been a neglected aspect of "critical zone" research [*Anderson et al*., 2007; *Brantley et al*., 2007; *Jin et al*., 2011; *Rempe and Dietrich*, 2014].

2. Methods

2.1. Site Description

The study site, "Rivendell" (39.729°N, 123.644°W, Figure 2) is located within the Angelo Coast Range Reserve in the Eel River watershed, approximately 260 km north of San Francisco. Rivendell includes an unchanneled, 4000 m^2 catchment that drains northward from the ridge (470 masl) to Elder Creek (392 masl), and a southward facing hillslope that drains toward the South Fork Eel River. Thin soils (10–30 cm thick near Elder Creek, and 30–70 cm thick at the divide) lie over a 2–4 m thick saprolite, and a weathered fractured bedrock zone that thickens toward the divide where it reaches to approximately 25 m in depth. The weathered bedrock is composed of vertically dipping beds of argillite with multiple, thin (typically multi-cm scale) sandstone interbeds, the most prominent of which forms the eastern ridge of the study area. The lithology is composed of turbidite sequences of the Coastal Belt of the Franciscan Complex [e.g., *Langenheim et al*., 2013]: low-grade, arkosic metagraywacke and argillite. *Langenheim et al*. [2013] refer to the geology as both shale and argillite. Here we adopt the original naming convention, argillite, as used in the construction of the regional geologic map [*McLaughlin et al*., 2000]. Illite, Fe-rich chlorite, kaolinite and mixed layer illite/montmorillonite are the major clay minerals, and the major primary minerals are quartz K-feldspar, plagioclase and chlorite [*Kim et al*., 2014].

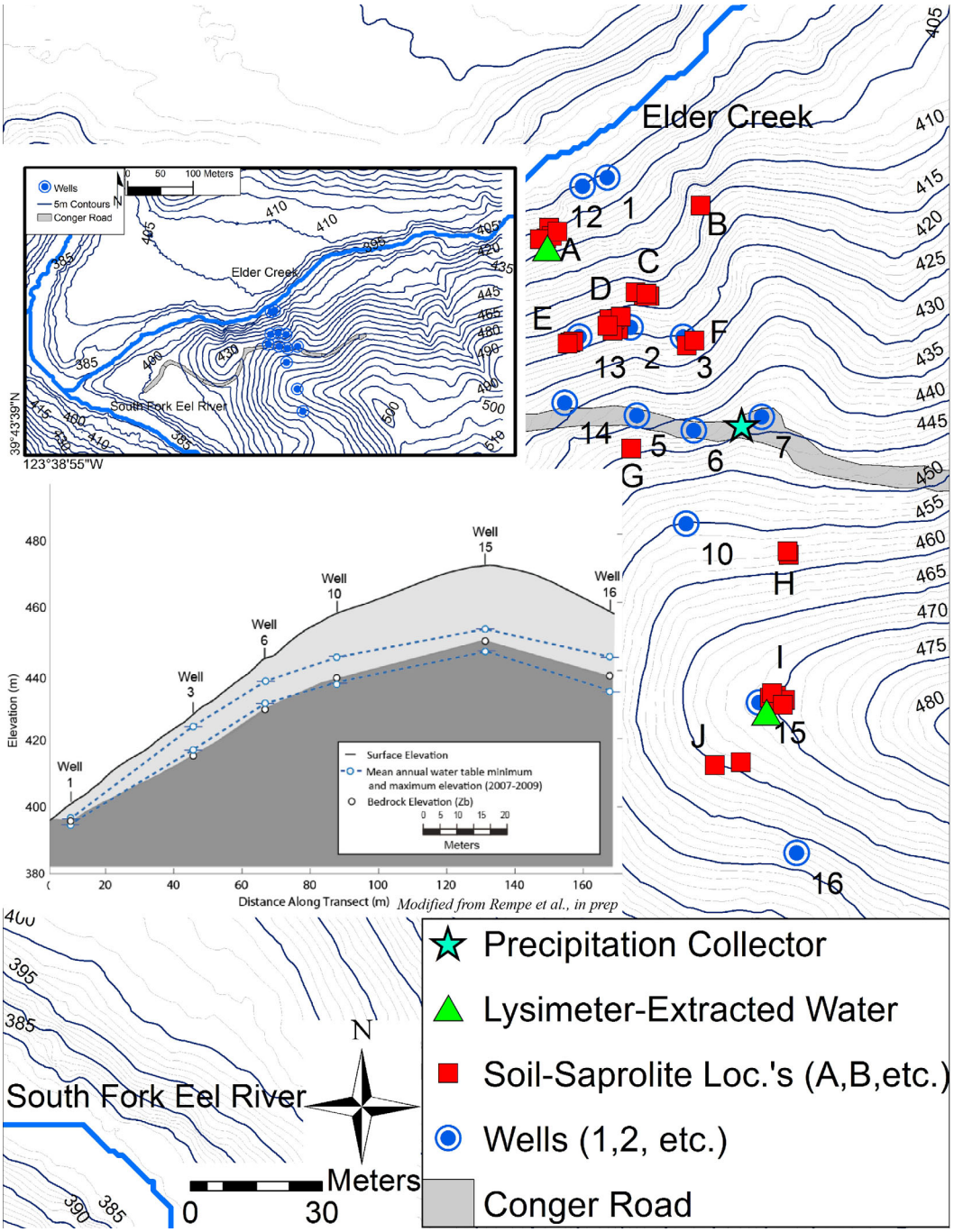

Figure 2. The Rivendell study site (39.729 N, 123.644 W), which lies within the Angelo Coast Range Reserve, in Northern California. Elder Creek lies at the base of the hillslope, and flows west, toward the South Fork of the Eel River, approximately 400 m downstream. The map shows 1 m contour LiDAR generated by the National Center for Airborne Laser Mapping. Blue dots show the location of deep groundwater monitoring wells. Red squares show the location of bulk soil and saprolite sampling sites. Green triangles show the location of mobile water sampling. The cyan star indicates the location of precipitation collection.

Along the coast near the headwaters of the South Fork Eel, the uplift rate is about 0.4 mm/yr [*Fuller et al.*, 2009; *Merritts and Bull*, 1989]. In our study area channel incision rate may have been 0.4–0.5 mm/yr in the late Pleistocene but then reduced to Holocene it $\sim$ 0.2 mm/yr in the Holocence [*Fuller et al.*, 2009; *Willenbring et al.*, 2013]. There are numerous deep-seated landslides, many of which are likely inactive vestiges of the Pleistocene [*Mackey et al.*, 2009]. At the Rivendell site, the average gradient on the North

Slope is 32°, while the south slope, which is the headwall of a deep-seated landslide, is considerably shallower (25°).

The region has a Mediterranean climate with 1763 mm average annual precipitation (60 year average precipitation) falling between October and May (at nearby *Richardson Grove State Park Weather Station*, 2015). There is significant inter-annual precipitation variation. Summers are dry, and the site receives little fog. A perched water table sits above fresh closed-fractured bedrock that is chronically saturated [*Salve et al*., 2012]. The elevation at the transition to fresh bedrock we refer to as Z_b [*Rempe and Dietrich*, 2014], which was determined by geophysical techniques, core logs, and seasonal water table dynamics. The site is vegetated by old-growth mixed canopy forest of Douglas-fir (*Pseudotsuga menziesii*), coast redwood (*Sequoia sempervirens*), Pacific madrone (*Arbutus menziesii*), Interior Live Oak (*Quercus wislizenii)*, California bay laurel (*Umbellularia californica)*, tanoak (*Notholithocarpus densiora)*, and a riparian corridor of big leaf maple (*Acer macrophyllum)*, and alder (*Alnus rhombifolia)*.

Rivendell is an intensively instrumented site. Over 700 instruments record the flow and content of water from the atmosphere into the subsurface, up into vegetation, and down to the water table. Twelve monitoring wells (Figure 2) measure a dynamic, perched groundwater. Seven wells were installed in 2007 by way of dry augering. An additional 5 wells were similarly drilled and installed in August 2010. The water table fluctuates with seasonal precipitation inputs, and has a dynamic range of 3–5 m below ground near Elder Creek to 18–25 m below ground at the ridge. We observe no overland flow and all runoff on our hillslope is generated from rainfall passing through the weathered bedrock [*Salve et al*., 2012]. In October 2011, we installed five 30 cm long moisture probes (two rod, CS650 soil reflectometer, Campbell Scientific, Logan Utah) at location I (and well 15) on the ridge top (Figure 2) by digging a pit, installing probes and back filling with the displaced native materials. We installed probes horizontally into undisturbed soil at depths of 15 and 35 cm. We also installed probes horizontally into undisturbed saprolite at depths of 70 and 100 cm, and one probe was installed vertically into undisturbed saprolite at 138–160 cm depth. The probes were calibrated for granular soils. Because our instruments were installed into soil, and saprolite, the instruments were field calibrated using gravimetric moisture measurements. *Oshun* [2016] shows a well-correlated relationship between instrument-measured permittivity and independently determined gravimetric moisture content.

2.2. Sample Collection and Analysis

Precipitation was measured with TE525 Tipping Bucket Rain Gages (Campbell Scientific, Logan, UT) tipping bucket rain gages on site beneath the canopy as well as in the meadow across Elder Creek. Daily precipitation samples were collected from a mineral oil capped container positioned beneath the canopy (cyan star in Figure 2). Precipitation samples were collected in 50 mL Nalgene HDPE vials with no headspace, parafilmed (PPPC, Chicago), and refrigerated until analysis. Precipitation was also collected from meadow. No isotopic difference was seen between rainfall collected in the meadow and rainfall collected on site below the canopy. Precipitation amounts, recorded with tipping bucket gages below the canopy, were used to calculate the volume weighted average isotopic composition for individual storms. Dry periods of 8 h or more were used to divide individual storms.

In August 2010, weathered bedrock was sampled while dry augering to install wells 12, 13, 14, 15, and 16 (Figure 2). These samples were taken from depths of 1.5–30 m during Standard Penetration Tests, which measured the number of blows from a 120 lb. hammer required to generate an adequate sample. The fracture structure of the weathered rock was destroyed by the sampling method, but the dry drilling method preserved the water isotopic composition. Samples of weathered bedrock were collected in 4 mL scintillation vials (VWR International, Brisbane, CA), which were labeled, parafilmed, and frozen until cryogenic extraction and analysis.

Soil and saprolite samples were collected through the summer of 2010, and every 2–4 weeks from June 2011 to January 2013. A 6 cm bucket auger was used to sample soil and saprolite every 10 cm to a maximum depth of 130 cm. Soil and saprolite sampling locations were distributed throughout the hillslope so as to prevent excessive disturbance in one area (Figure 2), although at one location (A on Figure 2) 9 holes 40 cm apart were drilled 20 October 2010, a month after the first light rain of the Fall, but before the first major storm. In January 2013, we went to two separate spots, dug 0.70 m into the road cut corresponding to a distance of 1.5 meters below the overlying ground surface, in order to extract a block of sandstone

22 cm in diameter, and a block of argillite 31 cm in diameter. Analysis of all augered material reported in the subsequent section shows that no evaporative effects are found below the soil (a depth of 30–50 cm below the surface). These blocks of rock were taken from significant depth to avoid evaporative effects. After sampling the fine material on the outside of the two blocks, we measured distance from the exterior and cleaved pieces of the blocks using a hammer and chisel in order to sample sequentially from the exterior to the interior. Rock samples were broken and placed in 4 mL scintillation vials, labeled, parafilmed, and frozen until extraction and analysis. We repeated this measurement by digging out a 35 cm diameter block of argillite in February 2014. Soil, saprolite, weathered bedrock, fresh bedrock, and interior samples of sandstone and argillite were cryogenically extracted under vacuum at a temperature of 100°C for at least 1 h, following the protocol outlined in *West et al*. [2006]. Although the amount of water yield varied with the moisture content and the compaction of the soil, we estimate that 4 mL of soil or saprolite yielded between 200 μL and 1.5 mL of water. In the discussion section, we examine the effect of different extraction methods on isotopic composition and validate the methods of extraction used in this study.

Groundwater samples were taken by lowering a 4 mL scintillation vial attached to a water level recorder. Water was collected at the top of the water column. Care was taken to eliminate headspace in the vial. Samples were sealed, labeled, parafilmed, and refrigerated until analysis. Although not shown here, we did sample through the water column in the well and found no isotopic difference with depth. The consistency in isotope composition through the water column is supported by observations of wintertime precipitation that infiltrates the subsurface at a temperature that is cold relative to groundwater, and creates a thermal instability that leads to a well-mixed groundwater reservoir [*Kim et al*., 2014].

To sample shallow mobile water, we installed six 5 cm diameter PVC-ceramic cup lysimeters near Elder Creek, and 3 at the ridge top (Figure 2). The ceramic cups were installed in the soil at depths of 30–40 cm, and in the saprolite at depths of 50–100 cm. A vacuum pump with pressure gage (MityVac) attached to a polyurethane tube was used to lower the potential inside the airtight lysimeters to −75 kPa. This low suction traps highly mobile water and is far less tension than the soil water tensions of −3.0 MPa that lead to stomatal closure in madrones [*Morrow and Mooney*, 1974]. The mobile water samples were pumped out after 1–5 h of applied tension similar to *Landon et al*. [1999]. Lysimeter extracted water was collected before and after the first rain in 2010, and at 12 dates spaced every 2–4 weeks (during the rainy season) from 2012 to 2013.

All samples were processed at the Stable Isotope Facility at UC Berkeley. Samples were run through a Isotope Ratio Mass Spectrometer or a Isotope Ratio Infrared Spectrometer to generate δD and δ^{18}O in permil notation with δD or $\delta^{18}\mathrm{O} = \left(\frac{R_{sample}}{R_{standard}} - 1\right) \times 1,000$, where R is the ratio of the heavy isotope (D or ^{18}O) to the light isotope (H or ^{16}O), with the standard being VSMOW (long-term precision of 1.0 ‰ for δD, and 0.11‰ for δ^{18}O). D-excess is calculated according to d= δD-8*δ^{18}O [*Dansgaard*, 1964].

3. Results

3.1. Cumulative Precipitation δD and Groundwater Response

Figure 3a shows the δD for individual storms from 2008 to 2012 and the volume-weighted average δD of total precipitation for 5 water years as a function of cumulative mm of rainfall. As the rainy season progresses, the cumulative volume-weighted average δD fluctuates less and trends toward the annual weighted average. Across the 5 years of observations, the volume-weighted average δD is −48.5‰ (the average is slightly different for different years). Figure 3b shows, for each water year, the volume-weighted average δD as a function of the cumulative precipitation necessary for a well to rise to 10% of its annual maximum rise. Individual storm values, as before, are also shown. The threshold of 10% of a well's annual rise marks the approximate transition from a hydrologic regime in which individual wells show a small sporadic response to rainfall across the hillslope, to one in which cumulative unsaturated flow has reached the groundwater causing significant recharge and large rise of the water table. The wells lower on the slope, where the weathering zone is shallower (wells 1, 2, and 3), will rise to 10% of their annual maximum earlier in the wet season, when the volume-weighted average δD of rainfall deviates from the annual volume-weighted average of −48.5‰. Higher up the slope by the time wells have responded by a 10% rise, the δD of cumulative precipitation has reached its annual average and the well water matches this value.

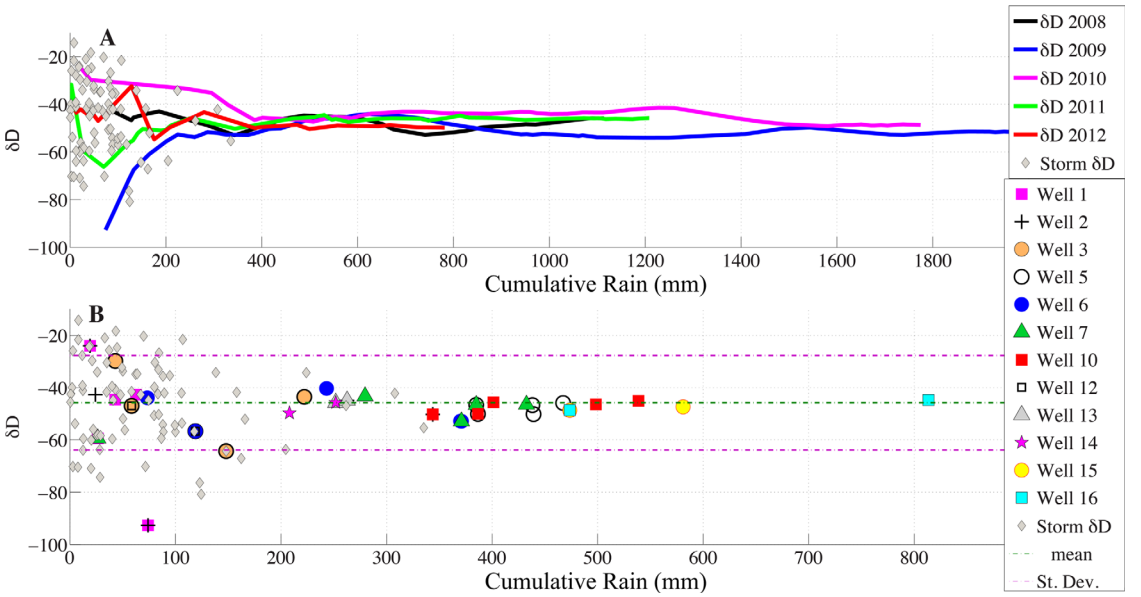

Figure 3. Precipitation δD for 5 years of observations. (a) Cumualtive, volume weighted δD of precipitation for 5 water years (colored lines for each water year) and individual average storm values (diamond symbols). (b) Cumulative rainfall required for each well to rise at least 10% of seasonal dynamic range plotted with storm values shown in Figure 3a. Green line and the pink dashed bounds, show the average and standard deviation in storm δD.

3.2. Isotopic Compositions of Subsurface Reservoirs

Figure 4 shows δ^{18}O and δD of precipitation and seven distinct water reservoirs derived from over 1200 samples spanning 3 years as well as the Local Meteoric Water Line (LMWL) fitted to the measured precipitation data, where $\delta D = 7.9\ \delta^{18}O + 12$. All data are included in Data Set S1 in the Supporting Information. Figure 5 shows that the data cluster into three main groups: (i) rock moisture, i.e., temporally dynamic bulk moisture extracted from saprolite (generally depths of 40–130 cm), weathered bedrock (depths of 3–35 m), fresh bedrock and rock interior, (ii) soil moisture (bulk moisture extracted from soil, depths of 0 cm up to 60 cm); and (iii) mobile waters (lysimeter extracted water, groundwater, and stream water) (Figure 5). The rock moisture falls close to but often

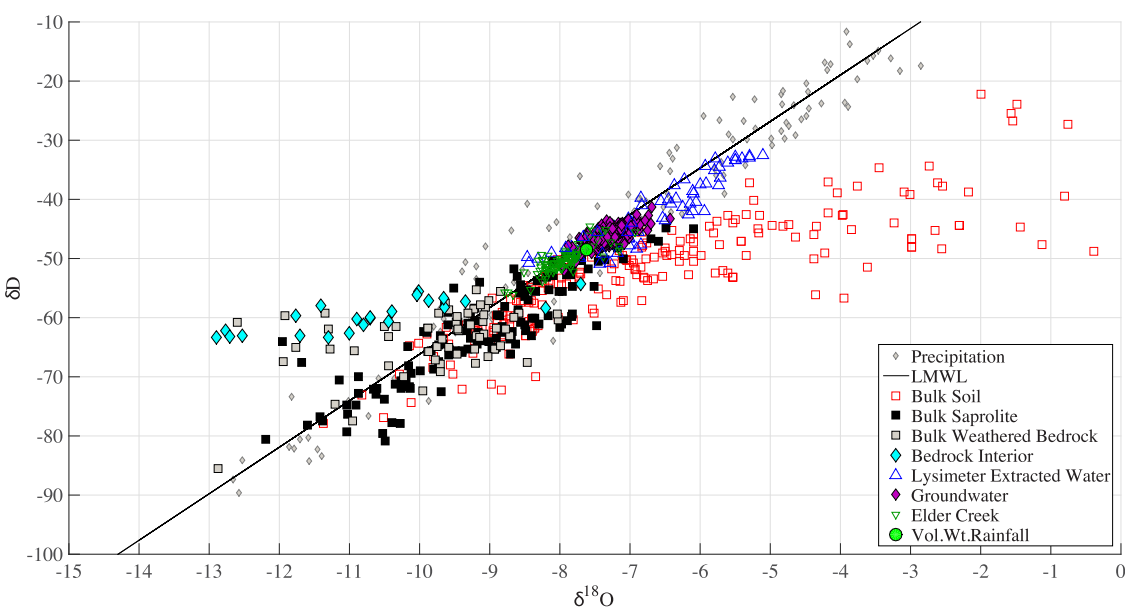

Figure 4. Stable isotope values of 7 water reservoirs (bulk soil, bulk saprolite, bulk weathered bedrock, interior bedrock, lysimeter-extracted (relatively mobile) water, groundwater, and Elder Creek runoff) relative to precipitation, represented by over 1200 data points. Solid line is LMWL ($\delta D = 7.9{*}\delta^{18}O + 12$). Volume weighted average rainfall for 2009–2013 is −7.62, −48.47‰ for ($\delta^{18}O$, δD) .

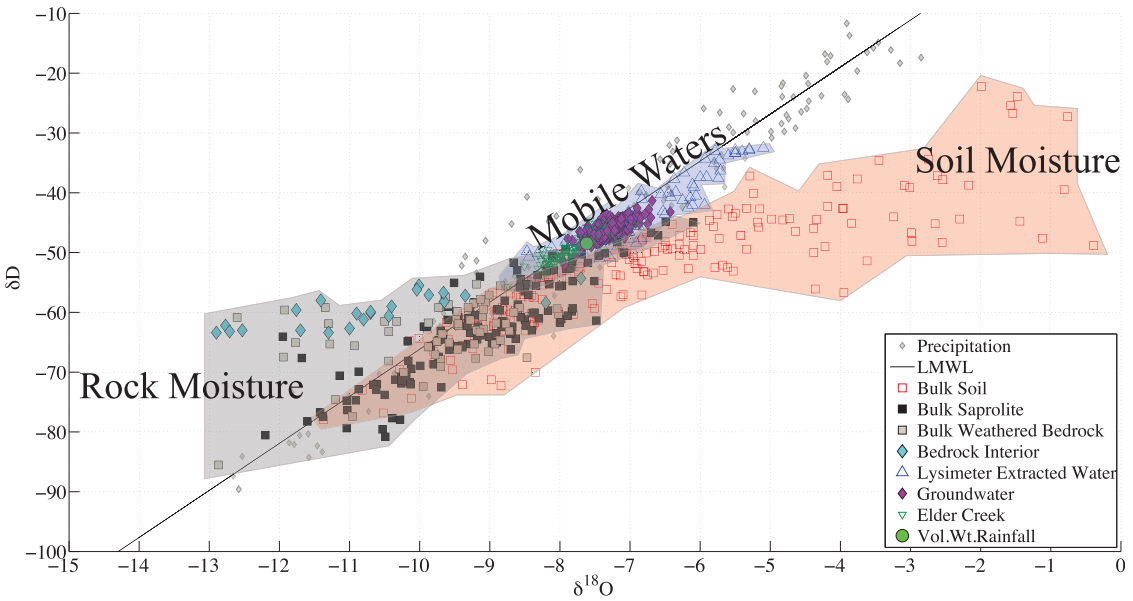

Figure 5. All data on LMWL with shaded areas encompassing all samples from the three main groups: mobile moisture (including lysimeter-extracted water, groundwater, and Elder Creek), soil moisture, and rock moisture (including saprolite, weathered bedrock moisture, and rock interior moisture).

slightly below the LMWL except for a local deviation centered on the bedrock interior moisture. Mobile water is enriched relative to rock moisture, with "Lysimeter Extracted Water" showing a large range, and groundwater and Elder Creek having small variations. The isotopic composition of the mobile water and groundwater is generally heavier than the average annual precipitation ("Vol. Wt. Rainfall") whereas Elder Creek is somewhat lighter. Soil moisture varies the most isotopically, with a large deviation from the LMWL due to evaporative enrichment during the summer dry season. The soil moisture ("Bulk Soil") isotopic compositions extend to very light isotopic compositions, (δD of $-80‰$), and the data lie slightly below, and at a lesser slope than the LMWL (along the expected evaporation line [e.g., *Dawson and Simonin*, 2012]).

Nearly all the rock moisture isotope compositions are lighter than the mobile waters, and they overlap with the deeper, isotopically lighter soil moisture values. Saprolite and weathered bedrock have similar isotopic compositions, but a portion of the weathered bedrock samples, collected during drilling to depths of up to 35 m to install the monitoring wells in 2010, lie well above the LMWL line (Figure 4). Moisture extracted from the interior of bedrock blocks distinctly fall well to the left of the LMWL. The bulk saprolite samples were obtained repeatedly throughout the year (soil/saprolite sites A-J in Figure 2), and varied seasonally in response to passage of mobile water in response to rains. Despite a wide range in precipitation inputs, water residing within the different subsurface materials has a distinctive and persistent isotopic composition *leading to an isotopically structured subsurface*.

Figure 6 shows a time series of the vertical structure of the isotopic compositions of water extracted from soil and saprolite at multiple locations across the hillslope. The soil-saprolite boundary is marked, and the locations are presented in the legend (which correspond to sampling locations in Figure 2). Date of the collection is marked at the top of each graph and the cumulative rain 30 days prior to that date is reported in the corner of each graph. The δD for that rain is marked with an inverted red triangle. Horizontal dashed lines indicate the depth of saprolite in each hole, colored to match the symbol of the location in the legend. At Location A (Figures 2 and Figure 6a), all the samples collected were adjacent to one another. Four of the plots (Figures 6a, 6b, 6d, and 6e) are at the end of summer or start of the wet season where little or no rain had occurred for over a month (total rains of 0, 3, 6 and 0 mm rainfall). On each of those days, the subsurface isotopic profile was similar at the different locations, with the shallow soil showing evaporative enrichment and the saprolite not showing evaporative enrichment. The local fine scale heterogeneity (Figure 6, Location A, 20 October 2010) is as large as the heterogeneity across the sites as expressed in comparison with Figures 6b, 6d, and 6e. Collectively these plots show that the saprolite was isotopically more negative at the end of the dry summer, with the value in 11 September 2011 distinctly lighter than that in the late

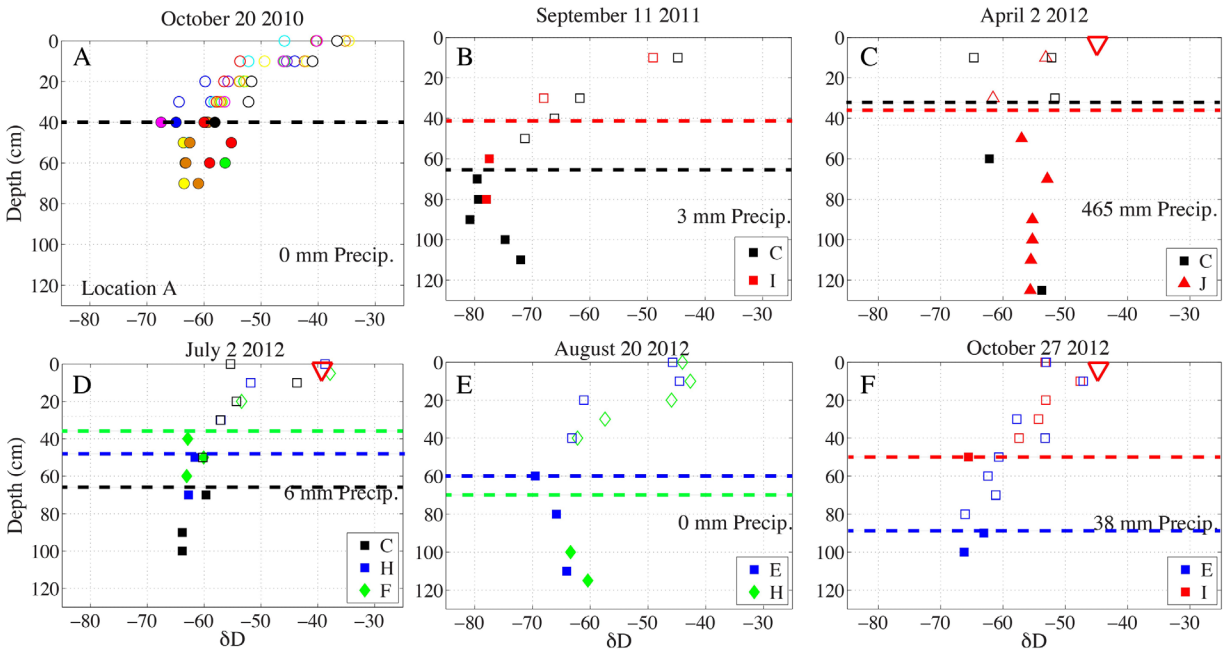

Figure 6. Bulk δD as a function of depth through the soil and saprolite at various sampling dates. Open symbols are soil, and closed symbols are saprolite. Date is indicated at the top of each plot. 20 October 2010 samples come from adjacent holes at site A (Figure 1). All other plots are from two to three locations from across hillslope with letter corresponding to location on Figure 2. Dashed horizontal lines (color coded for specific hole) indicate the depth of saprolite, and red triangle shows volumetrically weighted δD of previous rainfall (precipitation amount 30 days prior to sampling is included in each plot).

summer of August 2012. It appears that in the soil the evaporative enrichment is still visible even after the first 38 mm of rain in wet season that had fallen by 27 October 2012. Winter rains eliminate structure in the depth profile (2 April 2012), causing the saprolite to shift to a heavier value (even as it caused the soil profile to become lighter). Figure 7 shows histograms of δD for all soil and saprolite data collected over the period of 2011–2013. Winter bulk soil values show no vertical variation with depth in the soil, and δD varies (with three exceptions) from -65 to -45, a range that spans from much lighter than average annual precipitation, to just equal to the average annual precipitation. Winter soil is thus distinctly isotopically light. In contrast, the summer histogram shows the evaporative front to extend to no more than 30 cm depth. Winter bulk saprolite δD are similar to soil. However, in the summer, saprolite is distinctively light, centered on a value of $-60‰$.

Figure 8 shows δD values of precipitation and of each of the reservoirs from September 2009 to February 2013. Precipitation amount is shown in the top plot. The size of the precipitation symbols in the bottom plot is scaled by the size of the rainstorm event, and each year shows a distinctly different pattern of amounts and spread of δD values. The precipitation δD range varied widely during the of 2010–2011, and storms were far heavier in 2011–2012, and 2012–2013. Lysimeters were installed in September 2010, and used to collect soil and saprolite samples for the first storm of 2010. From October 2011 to January 2013, lysimeters were sampled after storm events when unsaturated zone mobile water was extractable at low tension. The "bulk weathered bedrock" samples were only taken in 2010 and the "interior" samples were only sampled in 2013 (2014 interior samples not shown on this plot). Figure 8 focuses on temporal variations hence spatial variations are not considered and all samples from the same reservoir type are treated collectively.

Broad patterns in the isotopic values of each reservoir reveal a dynamic structured heterogeneity. In Figure 9 each reservoir type is collectively labeled, and delineated. All boundaries were drawn by eye. The yellow blocks delineate the dry summer periods. There is a gap in the collection of bulk soil and rock samples between October 2010 and June 2011. The δD of precipitation, which can vary by as much as $80‰$ in a single storm, has an average value of $-48.5‰$, and a standard deviation of 21.6 $‰$ for the entire period of observation. The range in δD successively declined each year with far fewer isotopically light rains in the second and third year when the annual precipitation decreased. The volume weighted average δD of precipitation did vary annually: $-50.84‰$, $-48.76‰$, $-43.19‰$, and $-50.66‰$ for water years 2009, 2010, 2011, and 2012, respectively.

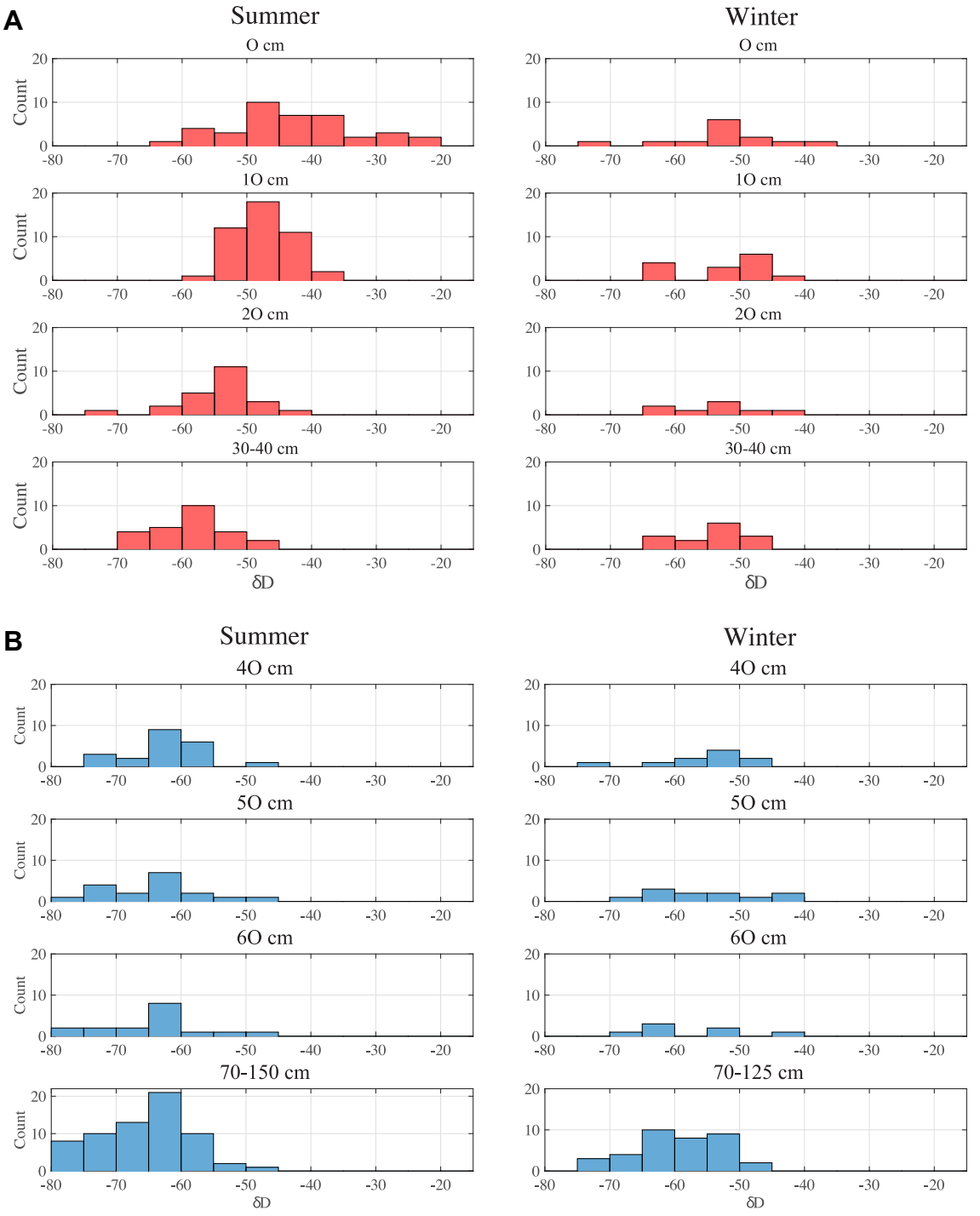

Figure 7. Histogram plots of δD of all (a) bulk soil moisture, and (b) bulk saprolite moisture as a function of depth. Data are divided between dry and wet season. In the dry season an evaporative front extends 30 cm into the soil. In the wet season, bulk soil moisture is mostly more negative than the average annual rainfall of $-48‰$. Bulk saprolite moisture shows no variation with depth and is distinctly negative in the dry season. In the wet season, bulk saprolite moisture becomes more positive, but, like soil moisture, is mostly more negative than average annual rainfall.

The lysimeter-extracted water (Figure 9) could only be collected during and shortly after selected rainstorms, otherwise this mobile fraction drained toward the water table, or was taken up by opportunistic tree roots. The δD of the lysimeter-extracted water (average $-43.8‰$, standard deviation $4.8‰$) reflects the recent precipitation inputs just prior to sampling. Lysimeter-extracted water represents the shallow soil and

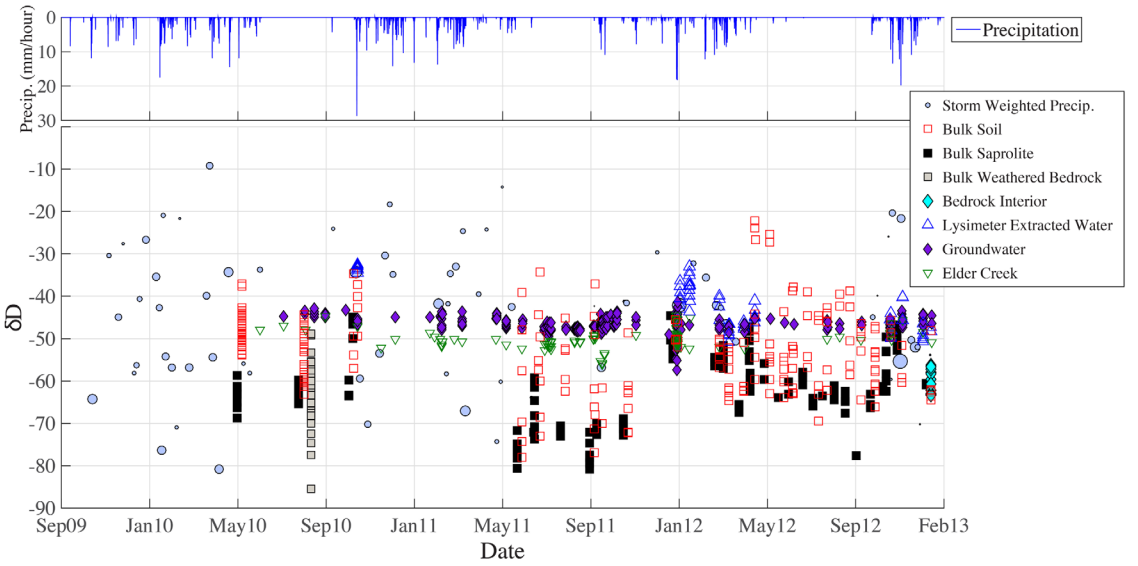

Figure 8. Time series of δD in the measured reservoirs from October 2009 to January 2013. Top plot shows hyetrograph, and bottom shows δD values across all reservoirs. Saprolite and soil samples from summer 2010 collected with Kevin A. Simonin, and presented in *Simonin et al.*, [2014].

saprolite reservoirs in which successive precipitation inputs mix. Mobile water drains through the weathered bedrock to the water table and enters the groundwater reservoir. The δD of all the groundwater samples fall within a narrow range of -43 to $-53‰$. The δD of groundwater, average: $-46.6‰$ (standard deviation $1.9‰$), is comparable to the volume weighted average precipitation (-48.5%), and is seasonally invariant. The δD of Elder Creek, average: $-50.3‰$ (standard deviation $2.2‰$), is consistently more negative than groundwater, and is also seasonally invariant. The Elder Creek samples are from the 16.9 km^2 basin which ascends to a height of 1290 m at the drainage divide, and summer low flow samples higher in the drainage suggest that the precipitation may be isotopically lighter (Lovill et al., 2015).

Mobile waters (lysimeter-extracted water, groundwater, and Elder Creek) thus show relatively stable values, with δD ranging from -52 to -32 and lying on and slightly below the LMWL (Figure 5). We attempted to document how an individual storm might send a transient signal in the mobile waters by collecting bi-hourly samples of precipitation, groundwater in three wells, and Elder Creek during a 308 mm storm event in January 2012. Figure 10 shows the hyetograph and isotopic composition of rainfall in the top two plots. The bottom 4 plots show the hydrologic response (in water height for the wells and in discharge in Elder

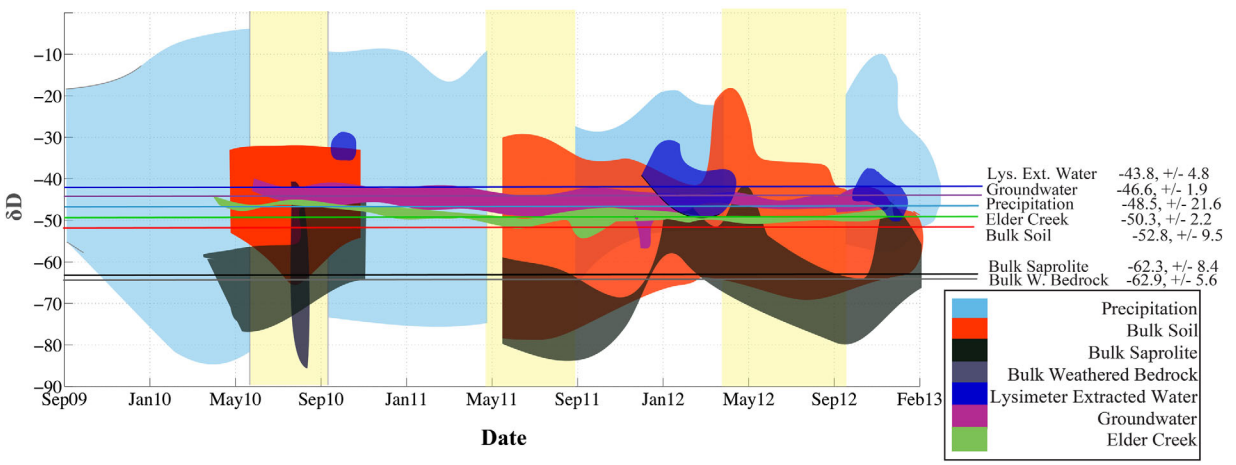

Figure 9. Dynamic structured heterogeneity of δD for the 7 reservoirs and precipitation. Colored areas were drawn by hand to encompass all δD values for a particular reservoir. Average values and dynamic ranges are shown on the right. From largest dynamic range to smallest: precipitation, bulk soil moisture, saprolite and deep rock moisture, soil and saprolite mobile water, Elder Creek, and groundwater. Shaded yellow vertical bars indicate summers, which have little to no precipitation.

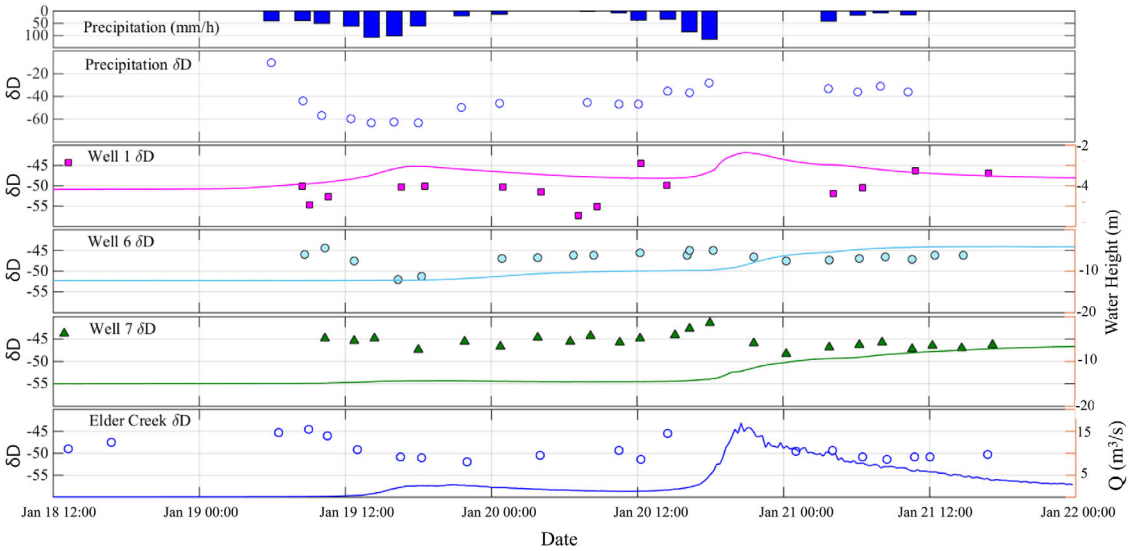

Figure 10. Hydrologic and isotopic response in wells 1, 6, 7, as well as Elder Creek to 308 mm of precipitation in January 2012. The upper two plots show a hyetograph of the storm and the δD of precipitation. The volume-weighted average of the storm was -6.84, $-42.19‰$ (δ^{18}O and δD). Scatter plot data are plotted against left y-axes, and shows variation in δD in precipitation, groundwater, and runoff. Hydrographs show the response of well water and Elder Creek, plotted against the right y-axes. Samples collected every 2–3 h for 55 continuous hours in January 2012.

Creek) on the right y-axes. The left y-axes show the δD of groundwater and of Elder Creek runoff through the storm. Precipitation inputs caused a 1 to 17 m rise in groundwater (responses of 1.5 to 8 m rise in wells shown here), and generated a large runoff response in the stream (peak discharge of 16.9 m^3/s, which exceeds bankfull discharge of 11 m^3/s). The δD of the precipitation was distinctly light in the first rain pulse then became heavier in the second. The storm yielded 308 mm of rain with a volume averaged δD of $-42.19‰$, heavier than the annual average of $-48‰$. Lysimeter extracted water was slightly enriched relative to average precipitation (-6.08, $-40.64‰$ in δ^{18}O and δD). Elder Creek δD did initially become lighter, perhaps in response to the first rain pulse, but the second heavier δD rain pulse did not cause the creek δD to change. Well 1, which is adjacent to Elder Creek, showed a hydrologic response in phase with the creek. The two wells 60 m upslope (wells 6 and 7–see Figure 2) showed a dull response to the first storm and then a delayed maximum response to the second wave of precipitation. Despite the hydrologic response seen below ground and in the stream, and variation in the δD in the wells and stream, there was only a fleeting increase in δD at well 7 at the beginning of the second pulse of rain. After this short isotopic change, well 7 continued to rise, but with an isotopic value indistinguishable from its prerain composition. Well 6 showed a δD response that was even more damped than well 7. Well 1, which is shallowest (Zb is nearest the surface), may respond to the rain δD, although the variance is large. The delayed response and the lack of an isotopic response to precipitation in the upslope wells and possible minor response at well 1 further illustrate that the temporal variation in the δD of precipitation is not transmitted through the hillslope to the channel.

Bulk samples of soil moisture showed the greatest isotopic range (Figures 5, 7a, and 9) of the subsurface reservoirs. The δD of bulk soil moisture, averaged $-52.8‰$ (standard deviation $9.5‰$) (Figure 9). Shallow evaporative enrichment in the dry season is revealed by samples that plot well to the right of the LMWL in Figure 5, and by the heavier δD values shown in the shallower soil (Figure 7). The histograms clearly show the wet season response of bulk soil moisture toward the value of incoming rainfall. Bulk samples collected immediately after rain include tightly held to lysimeter-extracted water. Evaporation effects are small in winter, and the bulk soil shows no evaporative front. Instead, the influx of precipitation homogenizes the bulk soil profile. However, the bulk soil remains to the negative side of precipitation inputs. In the winter, bulk soil plots near the LMWL, but slightly more negative than average annual rainfall, while lysimeter extracted water is slightly more positive than average annual rainfall (Figure 5).

The δD of bulk saprolite averaged $-62.3‰$ (standard deviation of $8.4‰$) as shown in Figure 9. For a given date, the multiple bulk samples record the vertical variation in δD, which is larger than the lateral spatial

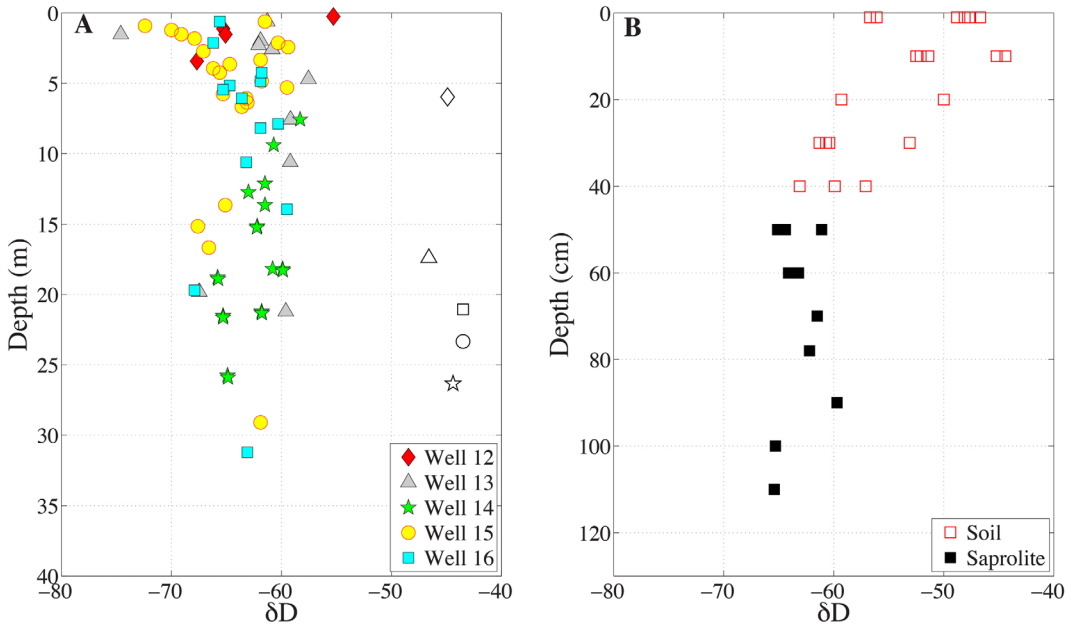

Figure 11. δD of bulk weathered bedrock as a function of depth below the surface. Samples taken during dry drilling and installation of 5 monitoring wells. Apart from well 12, the deepest sample at each well is in fresh bedrock, below Zb, and in the chronically saturated zone. Open symbols indicate the δD of groundwater at each well taken after drilling. Plot at right shows bulk δD through the soil and saprolite (collected with Kevin A. Simonin, published in *Simonin et al.*, [2014]).

variability shown at a specific location or between holes across the hillslope (Figure 6). Unlike the soil moisture, the saprolite moisture does not show evaporative enrichment, and plots below but nearly within the scatter of meteoric water close to the LMWL (Figure 5), but consistently lighter than the average δD of the rain (also visible in the Figure 7 histogram). The δD of the bulk saprolite, shown in black in Figure 9, although on average much lighter than other reservoirs, shows temporal swings during which it briefly approaches groundwater and precipitation, and then systematically becomes lighter, as the saprolite drains during the dry season.

The δD of deep weathered bedrock moisture, sampled in August 2010, is plotted against depth in Figure 11. Final well depth varied, with the deepest well reaching a depth of 35 m. These samples showed the same range and values as the bulk saprolite (Figure 9) and were significantly negative (average: $-62.9‰$) relative to precipitation and mobile as well as the bulk soil. Figure 11a plots the δD of the weathered bedrock with depth below the surface and compares with the groundwater (plotted as open symbols, and at the level at which groundwater was encountered during drilling). Individual well sites suggest there may be some local trend (perhaps getting lighter with depth at wells 12 and 14) but collectively no systematic variation is revealed. With the exception of well 12, the deepest sample was taken from fresh bedrock at or below the seasonal low of the water table, or Z_b. In all five cases, representing wells from adjacent to the channel to the ridge and beyond (well 16), the δD of the groundwater (open symbol) is far more positive than the collocated, surrounding weathered and fresh bedrock. Figure 11b shows the shallow soil and saprolite δD values at the same days the deeper cores were collected, and reveals that that the saprolite was isotopically similar to the deep weathered bedrock and showed no evidence of evaporative enrichment.

The isotopic compositions of bulk soil moisture and bulk saprolite are affected by the quantity of soil and saprolite moisture. Figure 12 shows variation in δ^{18}O, δD, and d-excess [*Dansgaard*, 1964] with moisture content for bulk soil and bulk saprolite samples. The color of each sample indicates the month of year in which the sample was collected. The moisture content was measured at the ridge top (Location I in Figure 2), and thus should not be viewed as absolute moisture content, but rather as an index of subsurface moisture at the time of sample collection. The depth of sample is paired with the appropriate moisture probe depth (15, 35, 70, 100, or 138 cm). The top row (Figures 12a–12c) shows variation in bulk soil isotopic composition as a function of moisture content. Bulk soil δ^{18}O and δD decrease slightly with increasing moisture content. Bulk soil d-excess is strongly dependent on moisture content, showing an evaporative effect when the soils are dry in late summer. The bottom row shows bulk saprolite isotopic composition as a function of

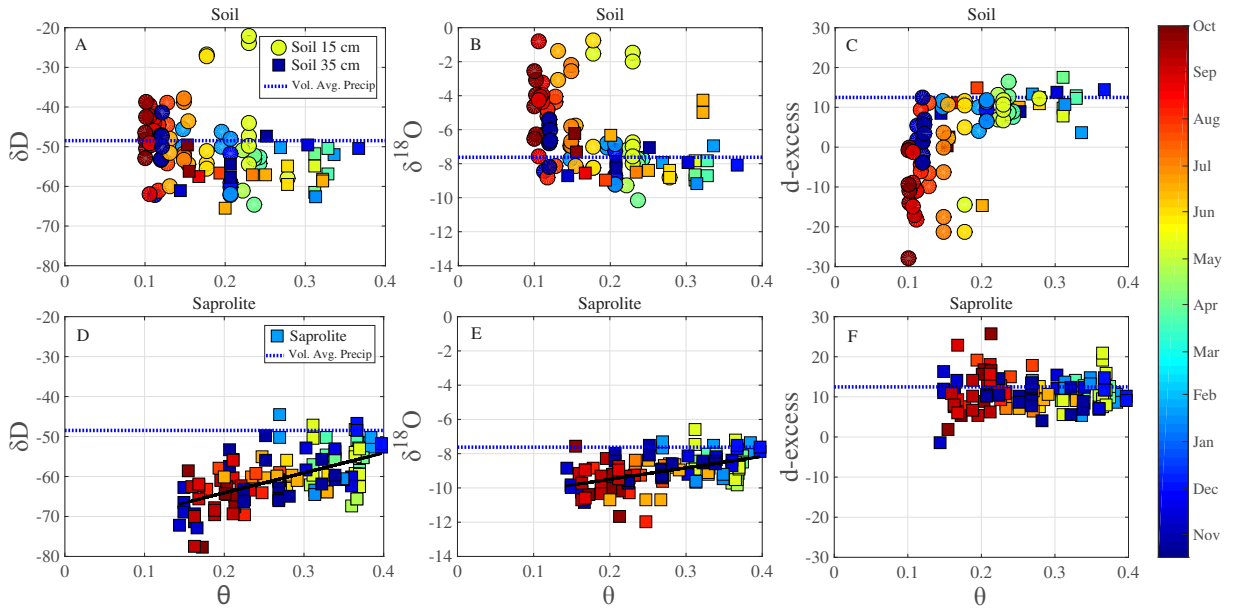

Figure 12. The relationship between soil and saprolite moisture content and the isotopic composition of bulk moisture in soil, and in saprolite. The color of the symbol represents the time of year during which the sample was collected, as indicated by the colorbar to the right. Bulk soil moisture δ^{18}O and δD show a weak negative trend to soil moisture content. Bulk soil moisture d-excess decreases with decreasing moisture content, pointing to a strong evaporative effect in the soil. A positive relationship exists between average saprolite moisture content and average saprolite δ^{18}O and δD (D and E). $\delta^{18}O = 6.67*\Theta - 10.83$ ($r^2 = 0.28$), and $\delta D = 49.93*\Theta - 74.07$ ($r^2 = 0.34$), At low moisture contents bulk saprolite δ^{18}O and δD are more negative, indicating tightly held moisture controls the negative isotopic composition measured in the bulk moisture.

saprolite moisture content. Bulk saprolite δ^{18}O and δD are lightest in the dry summer, and increase with moisture content, but remain more negative than average annual rainfall. Trend lines are drawn to show the relationship between moisture content and bulk saprolite δ^{18}O and δD. The isotopic composition of bulk saprolite moisture plots just below, but near the LMWL throughout the year. D-excess is thus near, but generally slightly below that of average precipitation, and does not vary with moisture content.

Figures 13a and 13b show the persistent structure to the isotopic composition of mobile and bulk waters. In Figure 13a, the δD of the bulk soil, bulk saprolite, the lysimeter samples ("mobile water" in the soil and saprolite) and groundwater, collected immediately following 8 storms, are plotted against volume-weighted δD of precipitation for the corresponding storm. Multiple bulk soil, saprolite, and lysimeter extracted water δD values were taken through the vertical profile. Apart from the bulk soil sampled after an isotopically light rain, $-58‰$ δD, the δD of the bulk saprolite and bulk soil are consistently isotopically negative relative to precipitation, even just after the rainfall. These bulk samples are a mixture of precipitation inputs (lysimeter extracted water) and antecedent moisture. In contrast, the lysimeter-extracted mobile water remains isotopically enriched relative to precipitation. For some of the samples, the enrichment was greater for lysimeter-extracted water in the soil than in the saprolite. The δD of the groundwater (taken from wells 1, 6, 7, 12, and 15) and bulk soil sampled after each storm did not vary with the δD of storm precipitation, while the lysimeter-extracted water in the soil and saprolite, and bulk saprolite δD show a weak positive relationship to the δD of precipitation.

Figure 13b shows the isotopic composition of the bulk soil and saprolite plotted against collocated, coeval mobile waters (lysimeter-extracted water, or groundwater) for the 8 storms (and also for the August 2010 deep drilling and well installation). Surprisingly, the δD of the bulk soil and saprolite remain negative relative to lysimeter-extracted water following each storm. In the same plot (Figure 13b) the fresh bedrock δD values for each well sampled at the greatest depth of the well (Well 12), or below Z_b (Wells 13, 14, 15, and 16) in August 2010 are plotted against, δD mobile groundwater at the same level in the same well at the time of sampling (data are shown in Figure 11). This also shows that even in the case where the bulk sample is taken beneath the groundwater table, the bulk rock water δD is much lighter than the mobile groundwater. Both of these observations shown in Figure 13b indicate a strong tendency for the more tightly held water (that influences the bulk δD values) to remain distinctly lighter than the mobile water that passes through the rock, either as unsaturated or saturated flow.

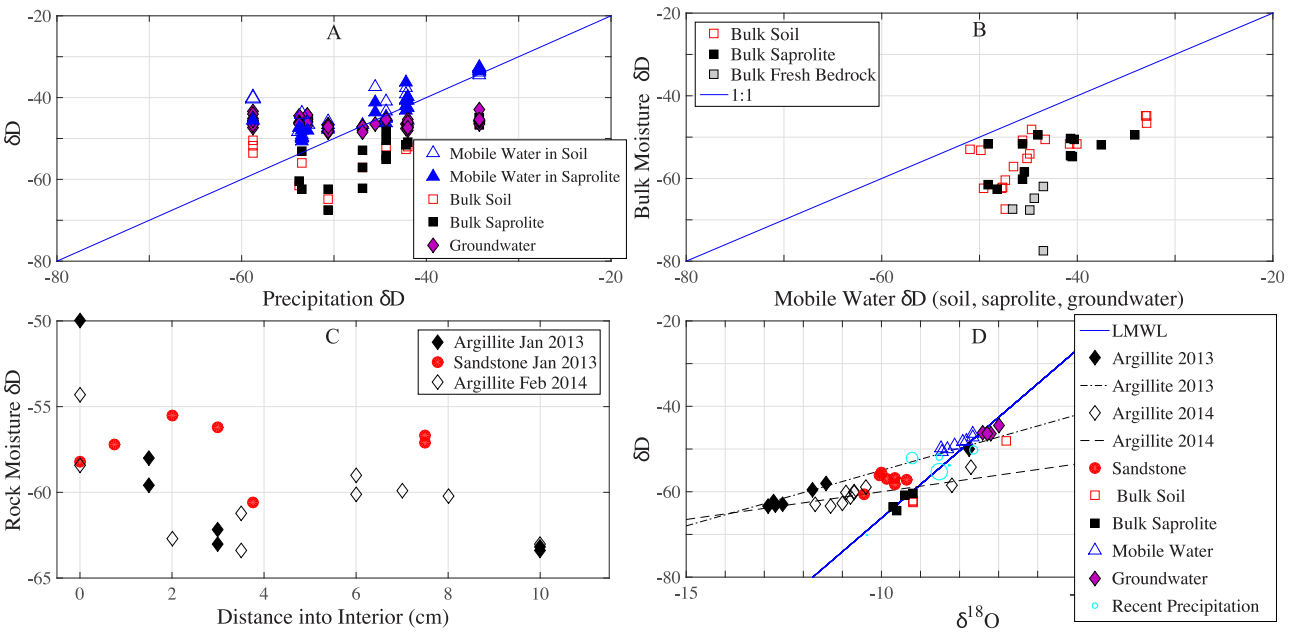

Figure 13. Variability in isotopic composition across different material properties and inside blocks of mudstone and sandstone. (a) Relationship between the volume weighted δD of precipitation and the δD of subsurface reservoirs measured immediately following the precipitation event. (b) Relationship between lysimeter-extracted water δD and bulk δD of soil, and saprolite. Also shown is δD of groundwater versus collocated bulk δD of fresh bedrock. Blue line in Figures 13a and 13b is a 1:1 line. (c) Bulk δD of interior mudstone and sandstone water as a function of distance from edge of weathered bedrock sample. (d) Interior weathered bedrock water with other reservoirs collected 14 January 2013. Interior mudstone δD falls to the left of the LMWL. Bulk saprolite δD is different than groundwater δD and lysimeter extracted δD. Also shown are mudstone interior samples from February 2014. Possible fractionation or mixing lines for 2013, and 2014 mudstone interior are shown with dashed lines. Slopes are 2.6 and 1.3 for 2013 and 2014, respectively.

To explore further this persistence and its possible origins, we analyzed the δD of samples from a 35 cm fracture-bordered block of argillite (extracted about 1.5 m below the surface) that was progressively broken to obtain interior samples. We subsequently compared that to a similar size block taken from a sandstone interbed in a large sandstone layer. Similarly, this block was taken from 1.5 m below the surface. Two blocks 1 year apart were analyzed of the argillite. Figure 13c shows that the δD of water from the argillite bedrock blocks decreases with distance from the surface of the block into the interior. Although water extracted from the fine grained material on the outside of the argillite block has an isotopic composition similar to bulk saprolite, the water just 2 to 3 cm to the interior of the block was more negative in both δD and δ^{18}O. As Figure 13d shows, the interior samples (argillite from two sampling periods, and sandstone from 2013) plot well to the left of the LMWL and are distinctly different from other subsurface reservoirs (Figure 13d). The trends of the two argillite blocks are similar. As shown in Figure 5, many of the argillite samples collected during the installation of wells in 2010 plot in the same field (to the left) relative to the LMWL as the bedrock interior samples. Sandstone outcrops on the eastern ridge of our study area and is present at a variety of scales throughout our site. In contrast to the argillite, sandstone interior samples were only slightly negative relative to the bulk sandstone saprolite sampled on the same day, and show no δD trend with distance into the bedrock interior.

4. Discussion

4.1. Isotopic Stability of the Groundwater and Elder Creek

Although the groundwater table shows a small rise in response to the first rainfall events of the Fall [*Salve et al.*, 2012], by the time the wells rise to 10% of their annual maximum, approximately 200–400 mm of precipitation has fallen, and the cumulative average δD of precipitation is similar to the annual volume-weighted average. Storm-based rock moisture monitoring shows that early storm water is injected into the weathered bedrock to depths of at least 1–2 m [*Salve et al.*, 2012], but that the entire hillslope does not become hydrologically responsive until about 400 mm of rain has fallen. Similar amounts of precipitation have been proposed to precede the generation of significant runoff in watersheds to the north of our field site [*Sayama et al.*, 2011]. Although storms often have isotopic variation that spans the entire LMWL, the

volumetrically weighted average δD of the larger storms, tends to be near the 5 year average of $-48.5‰$. The isotopic composition of large storms and the volumetrically weighted annual average rainfall appear to control the composition of the groundwater (Figure 3).

Figure 10 shows that despite isotopic variance, the δD in Elder Creek shows little response to the isotopic composition of the rainfall. There is a hint of an isotopic response, but no consistent trend in Elder Creek that would suggest the conservative passing of the isotopic composition of rainfall to the creek. Our findings differ from the many studies that have used hydrograph separation techniques to quantify the relative contributions of old (may include stream flow, groundwater, unsaturated zone moisture) and new water (precipitation) to storm runoff [e.g., *Sklash and Farvolden*, 1979; *McDonnell*, 1991; *Buttle*, 1998; *Klaus and McDonnell*, 2013]. Using a stable isotope hydrograph separation approach on storm flow in the Mattole River (60 km to the north, and predominantly within the Coastal Belt), *Kennedy et al*. [1986] concluded that precipitation passing through the soil was "buffered" due to extensive interaction with materials and antecedent moisture such that little change in isotopic composition was observed in the Mattole River, despite a 60 fold increase in discharge. Rivendell has thin soils, but a thick weathering zone of saprolite, and weathered bedrock ($\sim$ 4 m near the stream to $\sim$ 25 m near the divide). The groundwater is relatively deep, and the Mediterranean climate leads to large seasonal moisture dynamics through this unsaturated zone. When rains come in the fall, a large storage deficit must be overcome (200 to 400 mm of precipitation) before a significant response is registered in the upslope wells. Although Elder Creek and the downslope wells respond to earlier storms, the first rain events of the season primarily go into storage in the unsaturated zone. Successive rains build up a seasonal, dynamic unsaturated zone mobile-water reservoir. Storms enter this reservoir, and mix with antecedent moisture, thus damping the isotopic composition of individual rainfall events. During our monitoring period, only one bankfull event in Elder Creek occurred: 20–21 January 2012. During this bankfull event the δD of Elder Creek had a value of $-49.4‰$ in δD, similar to the volumetrically weighted average rainfall for the rainfall that had fallen up to the point of peak discharge, as well as for the year. An extremely large storm event would produce a greater hydrologic response. However, our data suggest that the δD of this precipitation would be similar to the volumetrically weighted average rainfall (Figure 3), the dynamically mixed mobile water, groundwater, and Elder Creek. The combination of dynamic mixing of successive storms, as well as the potential for exchange with water held under variable tensions, has the effect of destroying the isotopic composition of individual storms before the water becomes groundwater or runoff.

Many hydrograph separation studies have pointed to the large contribution of antecedent soil water to runoff [e.g., *DeWalle et al*., 1988; *McDonnell et al*., 1991; *Swistock et al*., 1989: *Buttle*, 1994; *Rice and Hornberger*, 1998]. At Rivendell, large components of unsaturated mobile moisture in soil, saprolite, and weathered bedrock are likely contributing to runoff, but the similarity in their isotopic composition to runoff prevents the application of hydrograph separation methods. Catchments that have thin weathering zones with low permeability bedrock that results in overland flow runoff pathways, and a shallow water table that is isotopically distinct from the precipitation input and the stream would allow for using hydrograph separation techniques to measure accurately the isotopic composition of pulses of rainfall contributing to runoff. However, even when conditions are favorable, the combined use of hydrochemical and hydrometric approaches are necessary to generate meaningful hydrograph separation results [*Rice and Hornberger*, 1998].

4.2. Isotope Systematics in the Subsurface

Figure 14 depicts semiquantitative vertical columns of the subsurface critical zone and shows the δD of bulk and mobile waters (including the groundwater) across three periods: August 2010, September 2011 and January 2012. Granular soil is shown over fractured and soil-like saprolite, which in turn, overlies fractured bedrock whose fracture density and degree of aperture opening decrease with depth. The weathered bedrock column is not shown in the second and third sample periods because deep samples were only obtained from drilling in August 2010. The cumulative precipitation (1774 mm and 512 mm) and the volume weighted δD (-47.9% and -45.2%) are shown between the first and second, and the second and third periods. The first two periods are near the end of the dry season and no lysimeter samples could be collected due to the low soil and rock moisture content (hence, no colored mobile water is shown). The third period, January 2012, includes lysimeter samples from the soil and saprolite, hence the colored layers indicating "mobile" δD values. The bulk soil values are shown for the appropriate depth at which the samples were collected. Bulk saprolite and weathered bedrock δD values are averaged to yield the isotopic

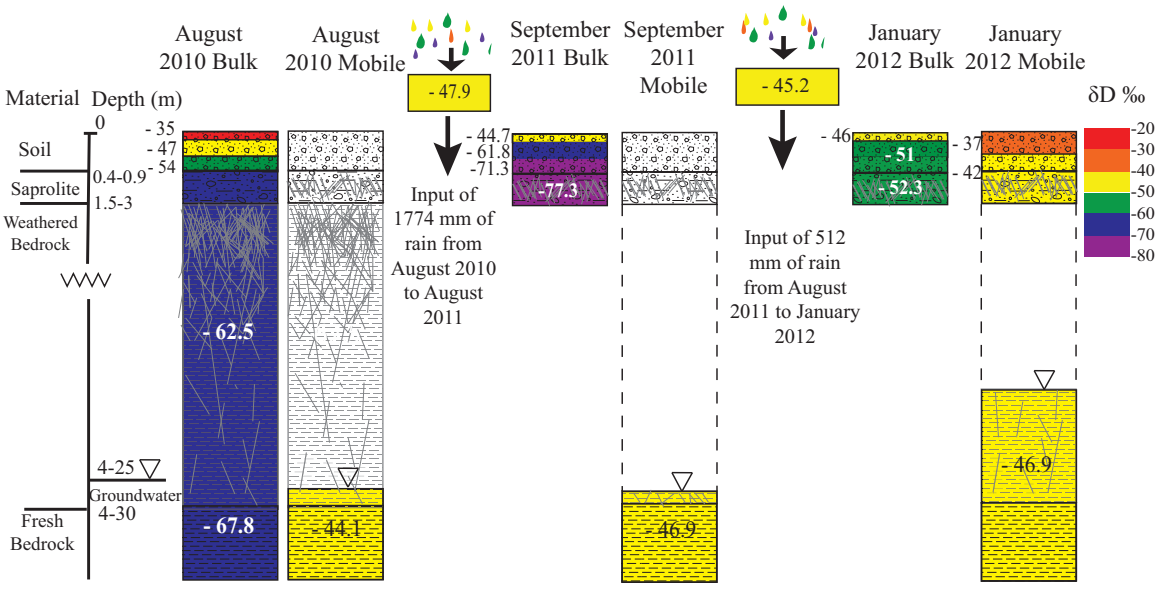

Figure 14. Semiquantitative illustration of mobile and bulk isotopic reservoirs. Three profiles from three different sampling periods show bulk reservoirs on the left and mobile reservoirs on the right. Deep drilling yielded bulk weathered and unweathered bedrock that was 20 ‰ lower than the mobile groundwater in δD. An evaporative front is seen in the soil of the August and September profiles. In wintertime, the bulk composition is affected by the input of precipitation and becomes heavier, however the mobile water is still 10 ‰ higher in δD than the bulk material through which it transits. Mobile water δD in the saprolite tends to be closer to the composition of groundwater than the mobile water in the soil and the volume weighted average rainfall than mobile water in the soil, which is more strongly affected by individual storms.

composition reported on this semiquantitative illustration. Saprolite is averaged over 40–130 cm depth (6–8 samples). There are no evaporative effects in the saprolite, and the changes in δD are relatively small.

As shown in Figure 14, in August 2010, relatively light δD in the weathered bedrock and saprolite was overlain by a bulk soil with a strong evaporative front toward the surface. The strongly negative δD of deep weathered saprolite and weathered bedrock rock moisture (−62.5% on average) was nearly the same as the shallow saprolite moisture (−63.3‰ on average). As Figure 4 illustrates, most of the shallow saprolite samples collected over 3 years, as well as the one-time deep sampling, plot down the LMWL, and are chronically lighter than mobile water. The difference, however, between the deep weathered bedrock δD (−67.8‰) and the groundwater δD in which it lies (−44.1‰) is large (August 2010). This implies that the majority of the water extracted from the bulk fresh bedrock is in relatively tightly held pores and that the groundwater is mostly held in more open, but infrequent fractures. Essentially, we sampled a mixture, predominantly composed of "matrix" with smaller contributions from fractures when we removed core samples for analysis.

The September 2011 data in Figure 14 show an evaporatively enriched shallow bulk soil (δD of −44.7‰). Despite 1774 mm of rain with an average δD of −47.9‰, which was nearly identical to the groundwater δD, the saprolite δD decreased by the end of summer. By January 2012, 512 mm of rain had arrived with an average δD of −45.2‰. The precipitation caused bulk soil to migrate toward the LMWL, erasing the evaporative enrichment in the shallow soil. Also, the isotopic composition of the precipitation caused an increase in the isotopic composition of the deeper bulk soil and bulk saprolite (δD of −51‰ and −52.3‰). Despite this increase in the bulk soil and saprolite isotope compositions, the bulk moisture remains more negative than the mobile water, which has a δD of −42‰. The δD of the lysimeter samples and the groundwater were similar to the volume weighted precipitation.

Collectively, the three dates in Figure 14 show the bulk soil, saprolite, and weathered bedrock to be consistently much lighter than the mobile waters (represented by the precipitation, the lysimeter samples, and the groundwater). Some of the dynamics in the soil and shallow saprolite are driven by moisture content change (i.e., Figure 12), which reveals that more tightly held water is systematically isotopically lighter. This suggests that the tightly bound moisture (micropore, and films of water on fractures, etc.) is the source of the strongly negative isotopic composition in the saprolite and weathered bedrock.

Figure 12 shows that saprolite bulk isotopic composition varies with moisture content. Saprolite lies below the evaporative front, and thus these changes in isotopic composition cannot be attributed

Table 1. Isotopic Composition of Water Entering and Leaving the Saprolite

Θ (cm^3/cm^3)	$\delta^{18}O$ Wet	$\delta^{18}O$ Dynamic Water	δD Wet	δD Dynamic Water
0.1	−10.08		−69.08	
		−8.80		−59.09
0.2	−9.44		−64.09	
		−7.51		−49.11
0.3	−8.80		−59.09	
		−6.22		−39.12
0.4	−8.15		−54.10	
		−4.94		−29.14
0.5	−7.51		−49.11	

to evaporative enrichment. The evolution of the measured bulk isotopic composition of the saprolite necessitates a coeval evolution of the water that enters or leaves the system (i.e., the more mobile fraction of water). The isotopic compositions of the dynamically moving water can be calculated using a two-end member mixing model.

$$\delta D_{n+1}\theta_{n+1} - \delta D_n\theta_n = \delta D_r(\theta_{n+1} - \theta_n) \quad (1)$$

δD_{n+1} is the bulk isotopic composition of saprolite at time (n+1), when moisture content is θ_{n+1}. δD_r is therefore the isotopic composition of the water that enters or leaves the saprolite, which has moisture content equal to $\theta_{n+1} - \theta_n$. Solving for δD_r, the dynamic water, yields the following equation:

$$\delta D_r = \frac{\delta D_{n+1}\theta_{n+1} - \delta D_n\theta_n}{(\theta_{n+1} - \theta_n)} \quad (2)$$

In the case of drying saprolite, $\theta_{n+1} < \theta_n$, δD_r will represent the moisture leaving the saprolite, either through drainage, or through root uptake. If $\theta_{n+1} > \theta_n$, δD_r represents the water entering the saprolite. The trend lines in Figures 12d and 12e are used to calculate δD_n and δD_{n+1} at moisture content intervals of 0.1 from 0.1 to 0.5. The dynamic water that enters the saprolite during periods of wet-up, or leaves the saprolite during periods of dry out is calculated using equation (2). The results in Table 1 show the isotopic composition ($\delta^{18}O$ and δD) of this dynamic water.

The calculated isotopic composition of the water leaving the saprolite falls along the LMWL and matches the range of "mobile water" obtained from lysimeter-extracted moisture. These calculations show that not only does the isotopic composition of bulk saprolite moisture decrease with decreasing moisture content, but that the dynamic moisture also becomes increasingly negative with decreasing moisture content. This points to an isotopic gradient that is dependent upon the tension at which water is held. The strongly negative isotopic composition comes from water that is held at the highest tensions. The data thus require a mechanism by which the isotopic composition of moisture is dependent upon the tension at which it is held.

The persistence of the negative bulk isotopic composition of the winter soil and bedrock (saprolite, weathered and fresh) at all times, the limitation of evaporative enrichment to the soil, and the apparent mixing of incoming precipitation waters in the soil and saprolite lead to a systematic spatially structured heterogeneity between mobile and bulk waters through a hillslope. We use the term "structured heterogeneity" to emphasize that the isotopic composition of water shows systematic and persistent variation with reservoir type (mobile waters, and bulk soil, saprolite, weathered and fresh bedrock). Figure 15 shows the corresponding location of each of these isotopically distinct groups within the hillslope for the dry summer and the wet winter. Solid lines connect the dry season mobile and bulk isotopic reservoirs with their respective material properties, or mobile reservoirs within the hillslope. Dashed show that in the wet season the isotopic evolution of bulk soil water toward the LMWL, bulk saprolite moisture up the LMWL toward mobile water, and the presence of mobile water, which is similar to groundwater. The values of some of these reservoirs are clearly dynamic (precipitation, lysimeter values, soil moisture) while others are stable (groundwater, and possibly weathered bedrock).

4.3. Water Extraction and Fractionation

Most puzzling is the light isotopic values of bulk soil and rock despite large fluxes of heavier mobile water. One concern might be the method by which we obtain the bulk water samples for analysis. Several studies challenge the effectiveness of the cryogenic extraction method we used in obtaining all water from a given sample. In a comparison of extraction methods across 14 laboratories *Walker et al*. [1994] found large discrepancies in isotopic composition, particularly in samples of low water and high clay content. Although the authors recommended higher temperature in order to extract tightly bound water, they cautioned against liberation of mineral water. Water incorporated into the mineral structure may be released at temperatures above 105°C [*Savin and Hsieh*, 1998; *Sacchi et al*., 2000]. In a test of the vacuum distillation method

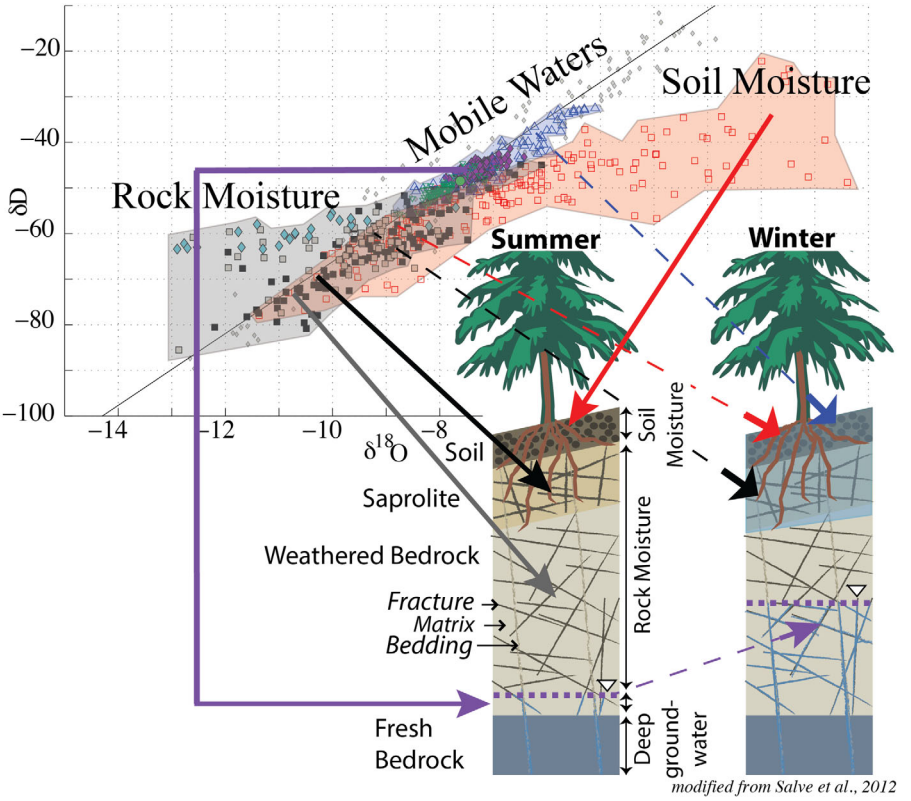

Figure 15. Location of different isotopic reservoirs within the hillslope. Lines connect the isotopic composition of the 3 main reservoirs with their location within a column representing the hillslope. Solid lines connect dry season isotopic composition of reservoirs with location in the hillslope. Dashed lines connect wet season isotopic composition of reservoirs with location in the hillslope.

Araguas-Araguas et al. [1995] found that insufficient temperatures or extraction times would lead to low-recovery samples that were more negative along a Rayleigh distillation curve. However, there is evidence that the clay material itself may cause isotopic fractionation due to weak bonding between water and clay [*Ingraham and Shadel*, 1992; see also *Oerter et al.*, 2014]. Other studies argue that cryogenic extraction at 100°C for more than 40 min is sufficient to obtain an unfractionated sample from clayey soils [*West*, 2006]. *Orlowski et al.* [2013] cite the importance of raising the temperature above 90°C, and remind us that the method of extraction may be designed to obtain water [sensu., *Tokunaga and Wan*, 1997; *Nimmo*, 2010] that is ecologically or hydrologically important, which does not include water bound into the mineral structure. In light of these concerns regarding the cryogenic extraction process, we tested our method to ensure recovery of an unfractionated sample. We cryogenically extracted two argillite bedrock samples, and one saprolite sample at 100°C for 1–6 h. Our goal was to extract all mobile, microporosity, and film water [*sensu.*, *Tokunaga and Wan*, 1997; *Nimmo*, 2010], but not the fixed water in the mineral structure. Although this more tightly held water might not rapidly contribute to stormflow generation, it is thought to be ecologically important water that is accessible to the matric pull of tree roots [*Brooks et al.*, 2010]. The argillite bedrock samples were collected from within the road cut, and the saprolite sample was collected from a depth of 70 cm at location I. Figure 16 shows δ^{18}O and δD as a function of extraction time (in hours) for saprolite and argillite bedrock, and gravimetric water yielded as a function of extraction time for the saprolite. We had fewer fresh argillite samples than saprolite samples. Mudstone samples were tested at 1, 3, and 6 h. Saprolite was tested at hourly intervals from 1 to 6. We measured gravimetric change only in the saprolite. Figure 16d shows the samples in dual isotope space, with color indicating the number of hours extracted. Although there is isotopic variation, apparent in the second argillite bedrock sample, there is no systematic offset indicative of a Rayleigh distillation effect due to incomplete extraction of water. We acknowledge that the absence of isotopic variation over the 6 h does not guarantee that we have extracted all microporosity, and film water. However, the absence of isotopic variation does strongly suggests that the remaining water, if present, represents a very small proportion of the total moisture, does not contribute

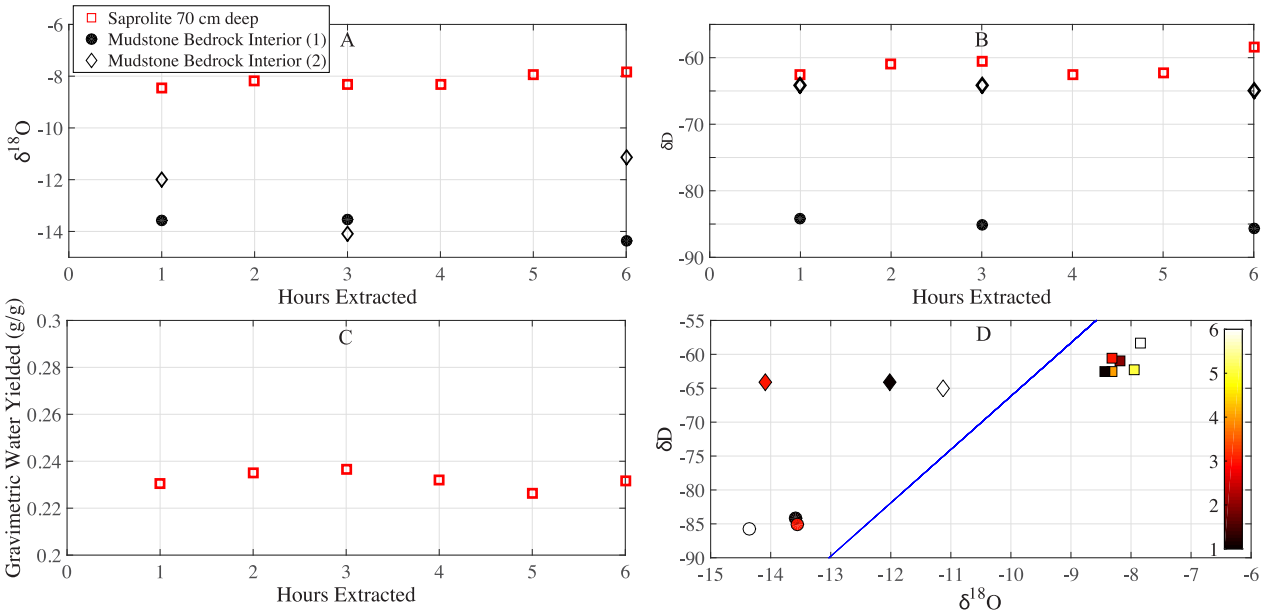

Figure 16. Test results justifying our cryogenic extraction methods. Top two plots show effect of cryogenic vacuum extraction time on δ^{18}O, and δD, for saprolite and weathered mudstone. Bottom left shows cryogenic vacuum extraction time vs. water yielded from saprolite. Bottom right shows all data plotted on LMWL with color indicating number of hours extracted.

significantly to the overall isotopic composition, and is likely not available to vegetation. There is no trend in the isotopic composition of water with extraction times beyond 1 h. Thus, we justify our extraction methods of 1 h, and focus on a discussion of the possible mechanisms producing the observed structured heterogeneity between mobile and bulk waters.

4.4. Mechanisms for the Persistently Negative Isotopic Composition of Bulk Moisture

First, we explore mechanisms that would lead to the persistently negative composition in the bulk saprolite, weathered bedrock, and non-evaporatively enriched soil. The offset between mobile and bulk (soil and rock) moisture occurs along the LMWL, similar to observed isotopic equilibrium fractionation associated with phase changes of water. Second, we discuss the observation that the isotopic composition of argillite interior water plots far to the left of the LMWL. We put forth testable hypotheses that may explain the persistence of strongly negative interior rock moisture.

The persistence of the offset between mobile and bulk moisture, which is more apparent at lower moisture contents, hints at a process beyond isotopic mixing. As noted in the introduction, limited data from other field sites suggest that the tension under which soil water is held might affect its isotopic composition. *Landon et al.* [1999] found that the freely mobile moisture (recharged from snowmelt) was isotopically more negative than more tightly held moisture in unsaturated sand. *Darling and Bath* [1988] observed that strongly negative winter storms generated a mobile groundwater isotopic composition that was more negative than bulk moisture extracted with a centrifuge from samples of chalk taken at the same depth. *Hsieh et al.* [1998] conducted laboratory tests that showed a positive correlation between bulk soil δ^{18}O and water content: we found a similar pattern in our bulk saprolite, but not bulk soil (Figure 12). *Hsieh et al.* [1998] hypothesized that different pools of water, from mobile to chemically adsorbed, had different thermodynamic properties, and correspondingly distinct isotopic compositions.

In soils measured in the field, systematically negative bulk soil moisture relative to lysimeter extracted soil water led *Brooks et al.* [2010] to reintroduce the idea of unsaturated zone moisture being held under a variety of tensions from mobile to immobile (MIM, in introduction) [e.g., *Biggar and Nielsen*, 1962; *De Smedt and Wierenga*, 1979; *Gvirtzman and Magaritz*, 1986]. *Brooks et al.* [2010] hypothesize that in a forested, Mediterranean climate, the first storms of the season will first fill shallow pores with isotopically heavy water, then deeper unsaturated layers with progressively light water (due to a rainout effect that coincides with the

sequential increases of moisture in an advancing wetting front). Although the authors do present data that show a wet up in the soil profile that corresponds in time with a rainout event in October 2006, there are no data that show how bulk soil water isotopes evolve with depth, and thus it is not possible for the reader to connect the data presented with their conceptual model (which could be explained by an evaporative soil front that develops in the dry summer). Furthermore, the data presented show that all lysimeter-extracted water is enriched (in both $\delta^{18}O$ and δD) relative to bulk water. This heavier mobile water presented in their data is at odds with the proposed conceptual model that requires an increasingly negative mobile water to recharge the tightly held water. A more complicated mechanism must be responsible for the isotopic difference between lysimeter-extracted water and bulk water.

We extend the observation that mobile water is enriched relative to bulk water [*Brooks et al*., 2010] beyond the soil and through the saprolite, weathered bedrock, and fresh bedrock. However, our data challenge the hypothesis put forward by *Brooks et al*. [2010]. We find no evidence that the isotopic composition of any one storm fills specific pore spaces in the depth profile. In fact, our data suggest that successive storms mix mobile water in the soil and saprolite before this water is fed into fractures and delivered to the water table to generate runoff (Figure 3). Furthermore, the isotopic composition of the bulk soil and saprolite (and presumably near-surface weathered bedrock) shifts back down the LMWL to more negative values as subsurface moisture levels decline after a rain event. The isotopic composition of this tightly held moisture (in both the deep soil and in the saprolite) retains an isotopically negative composition and does not record the meteoric signal of the successive storm events. This persistence points to the possibility of subsurface fractionation processes that mediate the isotopic composition of the rock and soil moisture.

Actively eroding soil and weathered bedrock will yield cations, which bind with water to form two concentric hydration spheres around the cation [e.g., *Feder and Taube*, 1952]. Experimental and theoretical studies show that the inner, tightly bound and highly structured sphere will concentrate the heavy isotopologues of water, while the loosely bound, less structured outer sphere will concentrate the lighter isotopologues of water [e.g., *Feder and Taube*, 1952; *Truesdell*, 1974; *Stewart and Friedman*, 1975; *Phillips and Bentley*, 1987; *Oerter et al*., 2014]. If the magnitude of fractionation in the inner sphere were of larger magnitude than in the outer sphere, more isotopically enriched water would be concentrated around the cation relative to the isotopically negative outer sphere. This would have the effect of fractionating the free water by preferentially taking more heavy isotopologues of water and binding them in the inner sphere around cations. At a mineral surface, where cations are produced due to weathering, this mechanism might have the effect of making the isotopic composition of the tightly held water more isotopically negative.

The presence of clay minerals that have low porosity, and adsorption sites for water and exchangeable hydroxyl groups may also affect the isotopic composition of bulk soil, saprolite, and weathered bedrock water. As water passes through a clay matrix, molecules can be adsorbed in two layers on the surface of the clay, an inner and an outer layer [*van Olphen*, 1965; *Sheppard and Gilg*, 1996]. Water molecules adsorbed to the inner clay layer require negative pressures exceeding 500 MPa to remove at 25°C [*van Olphen*, 1965]. Column experiments show that light isotopologues of water would preferentially bind to clays when passing through a dry, clay rich column of soil [*Araguas-Araguas et al*., 1995]. *Araguas-Araguas et al*. [1995] hypothesize that this observed fractionation was due to a "Rayleigh-type" fractionation process that resulted in isotopically negative bound water. *Oerter et al*. [2014] show that clay with high cation exchange capacity can produce an isotopic effect in free water due to fractionation associated with adsorption. Adsorption of water on the inner clay layer and the exchangeability of this adsorbed water with freely mobile water represent a process that is repeatable, and thus differs from the one-way filtration effect described below.

Kaolinite is known to have hydroxyl groups that exchange with meteoric water to produce poorly constrained isotope effects [*Halevy*, 1964]. Fractionation due to adsorption on clay surfaces has been measured and occurs rapidly in laboratory experiments [*Stewart*, 1967], and, through mass dependent isotopic exchange, was suggested to lead to characteristic tritium compositions in tightly held water of deep unsaturated loess profiles [*Gvirtzman and Magaritz*, 1986]. At Rivendell, kaolinite may represent 17–20% of the clay minerals in the weathered bedrock [*Kim et al*., 2014]. Additionally, *Kim et al*. [2014] found that chemical weathering in the unsaturated zone rapidly increases the cation concentration of infiltrating rainwater, thus increasing the pH and alkalinity of the mobile water, as well as delivering cations to the groundwater. The kinetics involved in the chemical evolution of water through weathering reactions in the soil, saprolite, and weathered bedrock might generate small isotope effects. Fractionation of oxygen has been measured

between water and species in the carbonic acid system [*Beck et al*., 2005]. Chemical weathering may lead to equilibrium isotope fractionation in the tightly held water within the small pores or in films adhering to the saprolite and weathered bedrock. The tightly held water would show fractionation from meteoric water, while the large volume of mobile water would dilute any observable isotopic effects.

4.5. Implications for Structured Heterogeneity in the Subsurface

Isotope effects that occurred as a result of chemical weathering would not only be of interest to studies that define the flows of meteoric water through critical zone, but also for paleosol studies that rely on the isotopic composition of hydrogen and oxygen in mineral phases to reconstruct paleoclimate. These paleosol studies rely on the assumption that once formed, clays residing at lower temperatures do not experience post-formation isotopic fractionation [e.g., *Savin and Epstein*, 1970; *Savin and Hsieh*, 1998; *Yapp*, *1987*, 1998; *Zheng*, 1998, *Horbe*, 2011]. The isotopic composition can then be used to reconstruct paleoclimate [e.g., *Bechtel and Hoernes*, 1990; *Delgado and Reyes*, 1996; *Tabor and Montañez*, 2005]. Measuring the mineral phase water requires purging all free and adsorbed water at temperatures above 105°C, and then analyzing the composition of the remaining structurally bound water [*Stewart and Friedman*, 1975; *Magaritz and Taylor*, 1976]. *Savin and Epstein* [1970] measured the fractionation factor between water and three clays, and found the fractionation between kaolinite and water, $\alpha_{\mathrm{min}-H_2O}$, to be 1.027 for oxygen, and 0.94 for hydrogen. Thus, the process of kaolinite formation has an associated fractionation factor. Relative to the meteoric water at the time of formation, kaolinite will be enriched in ^{18}O, yet depleted in D. The paleosol geothermometer literature argues that little postformational isotopic exchange occurs below 100°C [*O'neil and Kharaka*, 1976; *Sheppard and Gilg*, 1996]; however, there is some evidence of postformational exchange for hydrogen at low temperatures [*Bird and Chivas*, 1989]. Although we do not measure the mineral phase isotopic composition of kaolinite at Rivendell, our data suggest that isotope effects occur at the mineral-water boundary. If these isotope effects result in alteration of the isotopic composition of the mineral phase of clays, the underlying assumption of paleosol studies would have to be reconsidered.

4.6. Possible Mechanisms Explaining Why Argillite Interior Water Falls Far to the Left of the LMWL

The isotopic composition of interior argillite moisture plots well to the left of the LMWL (Figure 13c). The location of these samples relative to the LMWL is characteristic of a nonequilibrium fractionation event, or, alternatively, may be due to mixing with an undefined source that has a strongly negative δ^{18}O composition. Laboratory studies show that H_2O flow rates are higher than D_2O through micropores in carbon rods [*Huber et al*., 1956], and across a sulfanated polystyrene membrane [*Myagkov*, 1961]. Additionally, fractionation due to filtration was measured as water passed through a 35% porosity montmorillonite disc [*Coplen and Hanshaw*, 1973]. The ultrafiltrate, which passed through the disc, was isotopically more negative, while the residual water was more positive. The presence of cations, which causes a fractionation between coordination spheres and noncoordinated water will increase the magnitude of this filtration effect as hydrated ions are left in the residuum [*Coplen and Hanshaw*, 1973; *Feder and Taube*, 1952; *Stewart and Friedman*, 1975; *Phillips and Bentley*, 1987; *Oerter et al*., 2014]. The filtration mechanism was invoked on a continental scale to explain isotopic fractionation of deuterium in groundwater passing through shale micropores in Canada [*Hitchon and Friedman*, 1969]. Figure 13d shows possible fractionation lines between the residual mobile water on the outside of the block (plots on the LMWL) and the ultrafiltrate microporosity water of argillite (far to the left of the LMWL) with a slope of 2.6 (2013), or 1.3 (2014) in dual isotope space, consistent with the laboratory filtration experiments of *Coplen and Hanshaw* [1973]. If this occurs at Rivendell, however, it would require the infiltrating water to take a one-way trip, or for the presence of an undocumented internal drain that empties argillite interiors and allows them to recharge. Although this represents an unknown that is difficult to measure, a fractionation due to filtration through micropores nonetheless may contribute to the negative values found in argillite interiors.

Alternatively, the negative values of the interior argillite water and the observed isotopic structure through the argillite matrix may be due to incomplete mixing of meteoric and paleo-meteoric water. As the coupled processes of tectonic uplift and river incision bring saturated bedrock toward the surface, fresh bedrock crosses Z_b, (the fresh bedrock boundary on top of which the water table is perched) and begins to experience seasonal drainage, leading to fracturing, and consequent exchange of dynamic meteoric water with interior moisture [*Rempe and Dietrich*, 2014]. The isotopic composition of this inherited microporosity water is difficult to predict, but may record paleo-meteoric water (with a negative δ^{18}O) of saturated micropores

set by slow regional groundwater flow as the bedrock lay below Z_b. The degree to which the tightly held water reflects meteoric water would be a function of its time spent in the near-surface environment. *Hiscock et al*. [2011] postulated that diffusion coefficients dependent on the lithology will set the exchange between interior and meteoric water, with complete exchange resulting in interior water with an isotopic composition matching meteoric water. The isotopic gradient in low permeability argillite, from the most negative interior to the exterior water that reflects meteoric input is consistent with this hypothesis. The lack of isotopic gradient in sandstone may be due to its higher permeability and diffusivity, which allowed for a more complete replacement of paleo-water with contemporary meteoric water.

5. Conclusions

Together the data presented here show for the first time a deep and temporally extensive view of water isotope reservoirs inside a hillslope. The persistent isotopic differences between mobile and bulk moisture as annual pulses of meteoric water pass through the soil, saprolite, and weathered bedrock reservoirs at Rivendell suggest that material properties influence both the differential movement and retention of water, and, possibly contribute to subsurface fractionation processes. Mobile water mixes successive storm inputs within the soil and saprolite therein generating an isotopic composition that is similar to the seasonal average of rainfall, and destroying the isotopic signals of specific storms. The isotopic composition of the bulk moisture in all three material reservoirs is chronically more negative than the mobile water that generates runoff. The persistence of this difference between mobile and bulk water suggests the presence of a fractionation process occurring within the hillslope. The offset between bulk and mobile moisture occurs along the LMWL. As such, if this offset were due to isotopic fractionation, the process would be an equilibrium fractionation. We propose the following hypotheses that may explain the mechanism for isotopic fractionation occurring within the hillslope. (1) Chemical weathering yields cations that preferentially bind heavy isotopologues of water within hydration spheres. This process might result in water with higher δD and δ^{18}O values. (2) The presence of clay minerals may preferentially bind isotopically light isotopologues of water, thus depleting the δD and δ^{18}O of tightly held water, and increasing the δD and δ^{18}O of free water in a Rayleigh-type fractionation process. 3) Chemical weathering and the formation of clay minerals such as kaolinite may occur with an associated fractionation factor that decreases the δD and δ^{18}O of tightly held water, and increases the δD and δ^{18}O of freely mobile water. The positive correlation between moisture content and isotopic composition in the saprolite makes this hypothesis most likely.

The isotopic composition of pore water inside argillite blocks lies well to the left of the LMWL. We propose two possible explanations for the isotopic composition of this pore water. (1) Filtration of meteoric water through the low porosity clay matrix results in a nonequilibrium fractionation effect wherein pore water is progressively more negative with distance into the center of an argillite block. The filtration mechanism would require consistent flow in and out of the argillite block. (2) Uplift and river incision bring fresh, saturated bedrock into the near surface environment. As the bedrock weathers, meteoric water replaces paleo-water, producing a pattern of isotopic zonation in which pore waters near the edge of the block are more similar to meteoric water, and pore waters in the less weathered center of the block retain an inherited isotopic composition of paleo-meteoric water that is more negative isotopically. The discussion notes that we cannot explain the drainage scenario that would result in the persistence of isotopically negative argillite interior pore waters. Thus, the second hypothesis may be more plausible. Regardless, some of the bulk argillite bedrock and saprolite samples also plot to the left of the LMWL, pointing to the broad importance of this interior moisture in setting the bulk isotopic composition throughout the subsurface.

Collectively our data reveal a persistent structured heterogeneity of water reservoirs, each with its own distinct isotope composition. This structured heterogeneity, which tracks predictable changes in material properties associated with uplift, erosion, and weathering, may be common throughout hilly landscapes. The isotopic signatures of individual storms are completely erased in the deep unsaturated zone: neither runoff nor residual water inside the hillslope records these events. Vegetation that taps tightly held water deeper than just the soil, and subsurface runoff through the weathered bedrock will each reflect the influence of these isotopic reservoirs. The temporal and spatial persistence of these isotopic differences suggest that subsurface fractionation processes need to be considered.

Acknowledgments
This work was supported by the Keck Foundation as well as National Science Foundation CZP EAR-1331940 for the Eel River Critical Zone Observatory. The authors thank Peter Steel and Collin Bode for field assistance. Thank you to James and Harmony DeWolf, who collected the precipitation data on which the LMWL was constructed and to which all subsequent isotope data is referenced. Paul Brooks and Wenbo Yang provided valuable insight and support throughout the analyses of water for stable isotope composition at the Center for Stable Isotope Biogeochemistry (CSIB), UC Berkeley.

References

Anderson, S. P., W. E. Dietrich, D. R. Montgomery, R. Torres, M. E. Conrad, and K. Loague (1997), Subsurface flow paths in a steep, unchanneled catchment, *Water Resour. Res.*, *33*, 2637–2653.
Anderson, S. P., F. von Blanckenburg, and A. F. White (2007), Physical and chemical controls on the critical zone, *Elements*, *3*, 315–319.
Araguas-Araguas, L., K. Rozanski, R. Gonfiantini, and D. Louvat (1995), Isotope effects accompanying vacuum extraction of soil water for stable isotope analysis, *J. Hydrol.*, *168*, 159–171.
Asano, Y., T. Uchida, and N. Ohte (2002), Residence times and flow paths of water in steep unchannelled catchments, Tanakami, *Japan, J. Hydrol.*, *261*, 173–192.
Banks, E. W., C. T. Simmons, A. J. Love, R. Cranswick, A. D. Werner, E. A. Bestland, M. Wood, and T. Wilson (2009), Fractured bedrock and saprolite hydrogeologic controls on groundwater/surface-water interaction: A conceptual model (Australia), *Hydrogeol. J.*, *17*(8), 1969–1989.
Bechtel, A., and S. Hoernes (1990), Oxygen isotope fractionation between oxygen of different sites in illite minerals: A potential single-mineral thermometer, *Contrib. Mineral. Petrol.*, *104*, 463–470.
Beck, W. C., E. L. Grossman, and J. W. Morse (2005), Experimental studies of oxygen isotope fractionation in the carbonic acid system at 15°, 25° and 40°C, *Geochim. Cosmochim. Acta*, *69*, 3496–3503.
Bestland, E., S. Milgate, D. Chittleborough, J. VanLeeuwen, N. Pichler, and L. Soloninka (2009), The significance and lag-time of deep through flow: An example form a small, ephemeral catchment with contrasting soil types in the Adelaide Hills, South Australia, *Hydrol. Earth Syst. Sci.*, *13*, 1201–1214.
Biggar, J. W., and D. R. Nielsen (1962), Miscible displacement: II. Behavior of tracers, *Soil Sci. Soc. Am. Proc.*, *26*, 125–128.
Bird, M. I., and A. R. Chivas (1989), Stable-isotope geochronology of the Australian regolith, *Geochim. Cosmochim. Acta*, *53*, 3239–3256.
Bodin, J., F. Delay, G. D. Marsily (2003), Solute transport in a single fracture with negligible matrix permeability: 1. fundamental mechanisms. *Hydrogeology J.*, *11*, 418–433.
Bornyasz, M. A., R. C. Graham, and M. F. Allen (2005), Ectomycorrhizae in a soil-weathered granitic bedrock regolith: Linking matrix resources to plants, *Geoderma*, *126*, 141–160, doi:10.1016/j.geoderma.2004.11.023.
Brantley, S. L., M. B. Goldhaber, and K. V. Ragnarsdottir (2007), Crossing disciplines and scales to understand the critical zone, *Elements*, *3*, 307–314.
Brooks, J. R., H. R. Barnard, R. Coulombe, and J. J. McDonnell (2010), Ecohydrologic separation of water between trees and streams in a Mediterranean climate, *Nat. Geosci.*, *3*, 101–104.
Buttle, J. M. (1994), Isotope hydrograph separations and rapid delivery of pre-event water from drainage basins, *Prog. Phys. Geogr.*, *18*(1), 16–41.
Buttle J. M. (1998), Fundamentals of small catchment hydrology, Chapter 1 (1–49), in *Isotope Tracers in Catchment Hydrology*, edited by C. Kendall and J. J. McDonnell, vol. 839, Elsevier, Amsterdam, Netherlands.
Chen X., Z. Zhang, X. Chen, and P. Shi (2009), The impact of land use and land cover changes on soil moisture and hydraulic conductivity along the karst hillslopes of southwest China. *Env. Earth Sci.*, *59*(4), 811–820.
Coplen, T. B., and B. B. Hanshaw (1973), Ultrafiltration by a compacted clay membrane-I. Oxygen and hydrogen isotopic fractionation, *Geochim. Cosmochim. Acta*, *37*, 2311–2327.
Dansgaard, W. (1964), Stable isotopes in precipitation, *Tellus*, *16*, 436–468.
Darling, W. G., and A. H. A. Bath (1988), Stable isotope study of recharge processes in the English Chalk, *J. Hydrol.*, *101*, 31–46.
Darling, W. G., A. H. Bath, and J. C. Talbot (2003), The O & H stable isotopic composition of fresh waters in the British Isles. 2. Surface waters and groundwater, *Hydrol. Earth Syst. Sci.*, *7*(2), 183–195.
Dawson, T. E., S. Mambelli, A. H. Plamboeck, P. H. Templer, and K. P. Tu (2002), Stable isotopes in plant ecology, *Annu. Rev. Ecol. Syst.*, *33*, 507–559.
Dawson, T. E., K. A. Simonin (2011), The Roles of Stable Isotopes in Forest Hydrology and Biogeochemistry. *Forest Hydrology and Biogeochemistry: Synthesis of Past Research and Future Directions*, *216*, 137 pp.
Delgado, A., and E. Reyes (1996), Oxygen and hydrogen isotope compositions in clay minerals: A potential single-mineral geothermometer, *Geochim. Cosmochim. Acta*, *60*, 4285–4289.
De Smedt, F., and P. J. Wierenga (1979), Mass transfer in porous media with immobile water, *J. Hydrol.*, *41*, 59–67.
DeWalle, D. R., B. R. Swistock, and W. E. Sharpe (1988), Three-component tracer model for stormflow on a small Appalachian forested catchment, *J. Hydrol.*, *104*(1–4), 301–310.
Dixon, J. L., A. M. Heimsath, and R. Amundson (2009), The critical role of climate and saprolite weathering in landscape evolution, *Earth Surf. Process. Land*, *34* (11), 1507–1521.
Evaristo, J., S. Jasechko, and J. J. McDonnell (2015), Global separation of plant transpiration from groundwater and streamflow, *Nature*, *525*, 91–94.
Feder, H. M., and H. Taube (1952), Ionic hydration: An isotopic fractionation technique, *J. Chem. Phys.*, *20*, 1335–1336.
Fuller, T. K., L. A. Perg, J. K. Willenbring, and K. Lepper (2009), Field evidence for climate-driven changes in sediment supply leading to strath terrace formation, *Geology*, *37*(5), 467–470.
Gabrielli, C. (2011), The role of bedrock groundwater in rainfall-runoff response at hillslope and catchment scales, MS thesis, Oreg. State Univ., Corvallis, Oreg.
Green, E. G., W. E. Dietrich, and J. F. Banfield (2006), Quantification of chemical weathering rates across an actively eroding hillslope, *Earth Planet. Sci. Lett.*, *242*, 155–169.
Gvirtzman, H., and M. Magaritz (1986), Investigation of water movement in the unsaturated zone under an irrigated area using environmental tritium, *Water Resour. Res.*, *22*, 635–642.
Halevy, E. (1964), The exchangeability of hydroxyl groups in kaolinite, *Geochim. Cosmochim. Acta*, *28*, 1139–1145.
Hiscock, K. M, M. A. George, and P. F. Dennis (2011), Stable isotope evidence for the hydrogeological characteristics of clay-rich till in northern East Anglia, *Q. J. Eng. Geol. Hydrogeol.*, *44*, 173–189.
Hitchon, B., and I. Friedman (1969), Geochemistry and origin of formation waters in the western Canada sedimentary basin—I. Stable isoopes of hydrogen and oxygen, *Geochim. Cosmochim. Acta*, *33*, 1321–1349.
Horbe, A. M. C. (2011), Oxygen and hydrogen isotopes in pedogenic minerals-Implication s for paleoclimate evolution in Amazonia during the Cenozoic, *Geoderma*, *163*, 178–184.
Hsieh, J. C. C., S. M. Savin, E. F. Kelley, and O. A. Chadwick (1998), Measurement of soil-water d 18O values by direct equilibration with CO 2, *Geoderma*, *82*, 255–268.

Huber, M. E., E. A. Flood, R. D. Heyding (1956), The micropore flow of H_2O and D_2O through activated carbon rods. *Canadian J. Chem.*, *34.9*, 1288–1301.
Ichiyanagi, K., Y. Onda, O. Tomatsu, H. Iwashita, and K. Kato (1994), Determination of components of stormflow using water chemistry and isotope tracers in steep forested catchments underlain by different bedrocks, in *Proceedings of the International Symposium on Forest Hydrology*, pp. 569–576, Tokyo, Japan.
Ingraham, N. L., and C. Shadel (1992), A comparison of the toluene distillation and vacuum/heat methods for extracting soil water for stable isotopic analysis, *J. Hydrol.*, *140*, 371–387.
Jin, L., D. M. Andrews, G. H. Holmes, H. Lin, and S. L. Brantley (2011), Opening the "Black Box": Water chemistry reveals hydrological controls on weathering in the Susquehanna Shale Hills Critical Zone Observatory, *Vadose Zone J.*, *10*(3), 928–942.
Katsuyama, M., M. Tani, and S. Nishimoto (2010), Connection between streamwater mean residence time and bedrock groundwater recharge/discharge dynamics in weathered granite catchments, *Hydrol. Processes*, *24*(16), 2287–2299.
Kendall, C., D. H. Doctor, and M. B. Young (2014), Environmental Isotope Applications in Hydrologic Studies, In *Treatise on Geochemistry*, Second Edition, edited by H. D. Holland, and K. K. Turekian, vol. 7, pp. 273–327, Oxford, Elsevier.
Kennedy, V. C., C. Kendall, G. W. Zellweger, T. A. Wyerman, R. J. Avanzino (1986), Determination of the components of stormflow using water chemistry and environmental isotopes, Mattole River basin, California. *J. Hydrol.*, *84.1*, 107–140.
Kim, H., J. K. B. Bishop, W. E. Dietrich, and I. Y. Fung (2014), Process dominance shift in solute chemistry as revealed by long-term high-frequency water chemistry observations of groundwater flowing through weathered argillite underlying a steep forested hillslope, *Geochim. Cosmochim. Acta.*, *140*, 1–19.
Klaus, J., and J. J. McDonnell (2013), Hydrograph separation using stable isotopes: Review and Evaluation. *J. Hydrol.*, *505*, 47–64.
Kosugi, K., S. Katsura, T. Mizuyama, S. Okunaka, and T. Mizutani (2008), Anomalous behavior of soil mantle groundwater demonstrates the major effects of bedrock groundwater on surface hydrological processes, *Water Resour. Res.*, *44*, W09430, doi:10.1029/2006WR005859.
Landon, M., G. Delin, S. Komor, and C. Regan (1999), Comparison of the stable- isotope composition of soil water collected from suction lysimeters, wick samplers, and cores in a sandy unsaturated zone, *J. Hydrol.*, *224*, 45–54.
Langenheim, V. E., R. C. Jachens, C. M. Wentworth, and R. J. McLaughlin (2013), previously unrecognized regional structure of the Coastal Belt of the Franciscan Complex, Northern California, revealed by magnetic data, *Geosphere*, *9*(6), 1514–1529, doi:10.1130/GES00942.1.
Lovill, S., W. E. Dietrich, and W. J. Hahm (2015), Drainage from the critical zone: lithologic, aspect, and vegetation controls on the spatial extent of wetted channels during the summer dry seasons, Abstract #H23J-03 presented at 2015 Fall Meeting, AGU, San Francisco, Calif.
Mackey, B., J. J. Roering, and J. A. McKean (2009), Long-term kinematics and sediment flux of an active earthflow, Eel River, California, *Geology*, *37*, 803–806.
Magaritz, M., and H. P. Taylor, (1976), Oxygen, hydrogen and carbon isotope studies of the Franciscan formation, Coast Ranges, California. *Geochimica et Cosmochimica Acta*, *40.2*, 215–234.
Maloszewski, P., W. Rauert, W. Stichler, and A. Herrmann (1983), Application of flow models in an alpine catchment area using tritium and deuterium data, *J. Hydrol.*, *66*, 319–330, doi:10.1016/0022-1694(83)90193-2.
Maloszewski, P., W. Rauert, P. Trimborn, A. Herrmann, and R. Rau (1992), Isotope hydrological study of mean transit times in an alpine basin (Wimbachtal, Germany), *J. Hydrol.*, *140*, 343–360, doi:10.1016/0022-1694(92)90247-S.
Mayer, A., T. Sandman, M. Breidenbach (2008) Effect of flow regime on physical nonequilibrium transport in unsaturated porous media. *Vadose Zone J.*, *7*(3), 981–991.
McCaig, M. (1983), Contributions to storm quickflow in a small headwater catchment-–The role of natural pipes and soil macropores, *Earth Planet. Sci. Lett.*, *8*, 239–252.
McDonnell, J. J. (1990), A rationale for old water discharge through macropores in a steep, humid catchment, *Water Resour. Res.*, *26*, 2821–2832.
McDonnell, J. J., M. K. Stewart, and I. F. Owens (1991), Effect of catchment-scale subsurface mixing on stream isotopic response, *Water Resour. Res.*, *27*, 3065–3073.
McGuire, K. J., D. R. DeWalle, and W. J. Gburek (2002), Evaluation of mean residence time in subsurface waters using oxygen-18 fluctuations during drought conditions in the mid-Appalachians, *J. Hydrol.*, *261*, 132–149, doi:10.1016/S0022-1694(02)00006-9.
McLaughlin, R. J., et al. (2000), Geology of Cape Mendocino, Eureka, Garberville, and Southwestern Part of the Hayfork 30_60 minute quadrangles and adjacent offshore area, Northern California, U.S. Geol. Surv. Misc. Field Stud. MF-2336, Washington, D. C.
Merritts, D., and W. B. Bull (1989), Interpreting quaternary uplift rates at the Mendocino Triple Junction, Northern California, from uplifted marine terraces, *Geology*, *17*(11), 1020–1024.
Montgomery, D. R., W. E. Dietrich, R. Torres, S. P. Anderson, J. T. Heffner, and K. Loague (1997), Hydrologic response of a steep, unchannled valley to natural and applied rainfall, *Water Resour. Res.*, *33*, 91–109.
Morrow, P. A., and H. A. Mooney (1974), Drought adaptations in two evergreen sclerophylls, *Oecologia*, *15*, 205–222.
Myagkov, N. P. (1961), Colloid-Chemical and electrochemical properties of non-metallic coatings and their Protective Action, Master's Thesis, Rizhsk. Politeklm. Inst.
Neretnieks, I. (2006), Channeling with diffusion into stagnant water and into a matrix in series. *Water Resour. Res.*, *42.11*.
Nimmo, J. R. (2010), Theory for source-responsive and free-surface film modeling of unsaturated flow, *Vadose Zone J.*, *9*, 295–306.
Oerter, E., K. Finstad, J. Schaefer, G. R. Goldsmith, T. Dawson, and R. Amundson (2014), Oxygen isotope fractionation effects in soil water via interaction with cations (Mg, Ca, K, Na) adsorbed to phyllosilicate clay minerals, *J. Hydrol.*, *515*, 1–9.
Onda, Y., Y. Komatsu, M. Tsujimora, and J. Fujihara (2001), The role of subsurface flow runoff through bedrock on storm flow generation, *Hydrol. Processes*, *15*, 1693–1706.
O'neil, J. R., and Y. K. Kharaka (1976), Hydrogen and oxygen isotope exchange reactions between clay minerals and water, *Geochim. Cosmochim. Acta*, *40*, 241–246.
Orlowski, N., H. G. Frede, N. Brüggemann, and L. Breuer (2013), Validation and application of a cryogenic vacuum extraction system for soil and plant water extraction for isotope analysis, *J. Sensors Sensor Syst.*, *2*, 179–193.
Oshun, J. (2016), The isotopic evolution of a raindrop thorugh the critical zone. PhD Dissertation UC Berkeley, Berkeley, Calif.
Pearce, A. J., M. K. Stewart, and M. G. Sklash (1986), Storm runoff generation in humid headwater catchments 1. Where does the water come from?, *Water Resour. Res.*, *22*, 1263–1272.
Phillips, F. M., and H. W. Bentley (1987), Isotopic fractionation during ion filtration: I. Theory, *Geochim. Cosmochim. Acta*, *51*, 683–695.
Rempe, D. M., and W. E. Dietrich (2014), A bottom-up control on fresh bedrock topography under landscapes, *Proc. Natl. Acad. Sci. U. S. A.*, *111*, 6576–6581.
Rice, K. C., and G. M. Hornberger (1998), Comparison of hydrochemical tracers to estimate source contributions to peak flow in a small, forested, headwater catchment, *Water Resour. Res.*, *34*, 1755–1766.

Richardson Grove State Park Weather Station (2015). [Available at http://www.wrcc.dri.edu/cgi-bin/cliMAIN.pl?carich+nca.]
Rosenbom, A. E., P. R. Jakobsen (2005), Infrared thermography and fracture analysis of preferential flow in chalk. *Vadose Zone J.*, *4.2*, 271–280.
Russo, D., W. A. Jury, and G. L. Butters (1989), Proc International Symposium on Rock at Great Depth, Pau., *Water Resour. Res.*, *25*, 2076–2080.
Sacchi, E., J. L. Michelot, H. Pitsch, P. Lalieux, and J. F. Aranyossy (2000), Extraction of water and solutes from argillaceous rocks for geochemical characterisation: Methods, processes, and current understanding, *Hydrogeol. J.*, *9*, 17–33.
Salve, R., D. R. Rempe, and W. E. Dietrich (2012), Rain, rock moisture dynamics, and the rapid response of perched groundwater in weathered, fractured argillite underlying a steep hillslope, *Water Resour. Res.*, *48*, W11528, doi:10.1029/2012WR012583.
Savin, S. M., and S. Epstein (1970), The oxygen and hydrogen isotope geochemistry of clay minerals, *Geochim. Cosmochim. Acta*, *34*, 25–42.
Savin, S. M., and J. C. C. Hsieh (1998), The hydrogen and oxygen isotope geochemistry of pedogenic clay minerals: Principles and theoretical background, *Geoderma*, *82*, 227–253.
Sayama, T., J. J. McDonnell, A. Dhakal, and K. Sullivan (2011), How much water can a watershed store?, *Hydrol. Processes*, *25*, 3809–3908.
Sheppard, S. M. F., and H. A. Gilg (1996), Stable isotope geochemistry of clay minerals, *Clay Miner.*, *31*, 1–24.
Simonin, K. A., P. Link, D. Rempe, S. Miller, J. Oshun, C. Bode, W. E. Dietrich, I. Fung, and T. E. Dawson (2014), Vegetation induced changes in the stable isotope composition of near surface humidity, *Ecohydrology*, *7*(3), 936–949.
Šimunek, J., N. J. Jarvis, M. Th. van Genuchten, A. Gärdenäs (2003), Review and comparison of models for describing non-equilibrium and preferential flow and transport in the vadose zone, *J. Hydrol. 272*, 14–35.
Sklash, M. G., and R. N. Farvolden (1979), The role of groundwater in storm runoff, *J. Hydrol.*, *43*, 45–65.
Sklash, M. G., M. K. Stewart, and A. J. Pearce (1986), Storm runoff generation in humid headwater catchments: 2. A case study of hillslope and low-order stream response, *Water Resour. Res.*, *22*, 1273–1282.
Soulsby, C., R. Malcolm, R. Helliwell, R. C. Ferrier, and A. Jenkins (2000), Isotope hydrology of the Allt a' Mharcaidh catchment, Cairngorms, Scotland: Implications for hydrological pathways and residence times, *Hydrol. Processes*, *14*, 747–762, doi:10.1002/(SICI)1099-1085(200003)14:4<747::HYP970>3.0.CO;2-0.
Stewart, G. L. (1967), Fractionation of tritium and deuterium in soil water, in *Isotope Techniques in the Hydrologic Cycle, Geophys. Monogr. Ser., 11*, edited by G. E. Stout, pp. 159–168, AGU, Washington, D. C.
Stewart, M. K., and I. Friedman (1975), Deuterium fractionation between aqueous salt solutions and water vapor, *J. Geophys. Res.*, *80*, 38 12–38.
Swistock, B. R., D. R. DeWalle, and W. E. Sharpe (1989), Sources of acidic storm flow in an Appalachian headwater stream, *Water Resour Res.*, *25*, 2139–2147.
Tabor, N. J., and I. P. Montañez (2005), Oxygen and hydrogen composition of Permian pedogenic phyllosilicates: Development of modern surface domain arrays and implication for paleotemperature reconstructions, *Palaeogeogr. Palaeoclimatol. Palaeoecol.*, *223*, 127–146.
Tokunaga, T. K., and J. Wan (1997), Water film flow along fracture surfaces of porous rock, *Water Resour. Res.*, *33*, 1287–1295.
Tromp-van Meerveld, H. J., N. E. Peters, and J. J. McDonnell (2007), Effect of bedrock permeability on subsurface stormflow and the water balance of a trenched hillslope at the Panola Mountain Research Watershed, Georgia, USA, *Hydrol. Processes*, *21*, 750–769, doi:10.1002/hyp.6265.
Truesdell, A. H. (1974), Oxygen isotope activities and concentration in aqueous salt solutions at elevated temperatures: Consequences for isotope geochemistry, *Earth Planet. Sci. Lett.*, *23*, 387–396.
Van Genuchten, M. Th., and P. J. Wierenga (1976), Mass transfer studies in sorbing porous media, 1, Analytical solutions, *Soil Sci. Soc., Am. J.*, *40*, 473–480.
van Olphen, H. (1965), Thermodynamics of interlayer adsorption of water in clays. I. Sodium vermiculite, *J. Colloid Sci.*, *20*, 822–837.
Vitvar, T., and W. Balderer (1997), Estimation of mean water residence times and runoff generation by 18O measurements in a pre-Alpine catchment (Rietholzbach, eastern Switzerland), *Appl. Geochem.*, *12*, 787–796, doi:10.1016/S0883-2927(97)00045-0.
Walker, G. R., P. H. Woods, and G. B. Allison (1994), Interlaboratory comparison of methods to determine the stable isotope composition of soil water, *Chem. Geol.*, *111*, 297–306.
Wang, J., M. Jin, and F. Kang (2015), Hydrochemical characteristics and geothermometry applications of thermal groundwater in northern Jinan, Shandong, China, *Geothermics*, *57*, 185–195.
West, A. G., S. J. Jackson, and J. R. Ehleringer (2006), Water extraction times for plant and soil materials used in stable isotope analysis, *Rapid Commun. Mass Spectrom.*, *20*, 1317–1321.
Willenbring, J. K., N. M. Gasparini, B. T. Crosby, and G. Brocard (2013), What does a mean mean? The temporal evolution of detrital cosmogenic denudation rates in a transient landscape, *Geology*, *41*(12), 1215–1218.
Wilson, C. J., and W. E. Dietrich (1987), The contribution of bedrock groundwater flow to storm runoff and high pore pressure development in hollows, *IAHS Publ.*, *165*, 49–59.
Yapp, C. J. (1987), Oxygen and hydrogen isotope variation among goethites (α-FeOOH) and the determination of paleotemperatures, *Geochim. Cosmochim. Acta*, *51*, 355–364.
Yapp, C. J. (1998), Paleoenvironmental interpretation of oxygen isotope ratio in oolitic ironstone, *Geochim. Cosmochim. Acta*, *62*, 2409–2430.
Zhao, P., X. Tang, P. Zhao, C. Wang, and J. Tang (2013), Identifying the water source for subsurface flow with deuterium and oxygen-18 isotopes of soil water collected from tension lysimeters and cores, *J. Hydrol.*, *503*, 1–10.
Zheng, Y.-F. (1998), Oxygen isotope fractionation between hydroxide minerals and water, *Phys. Chem. Miner.*, *25*, 213–221.